

Stability Analysis and Controller Tuning

CHAPTER

10

10.1 ■ INTRODUCTION

To this point, we have developed a control algorithm (the proportional-integral-derivative controller) and a method for tuning its adjustable constants. One might ask, “Isn’t this sufficient for designing feedback control systems?” The answer is a resounding “No!”, because we do not have a general method for evaluating the effects of elements in the closed-loop system on dynamic stability and performance.

Through various examples and exercises, we have seen how feedback control can change the qualitative behavior of a process, introducing oscillations in an originally overdamped system and potentially causing instability. In fact, we shall see that the stability limit is what prevents the use of a very high controller gain to improve the control performance of the controlled variable. Therefore, a thorough understanding of the stability of dynamic systems is essential, because it provides important relationships among process dynamics, controller tuning, and achievable performance. These relationships are used in a variety of ways, such as selecting controller modes, tuning controllers, and designing processes that are easier to control.

10.2 ■ THE CONCEPT OF STABILITY

In vernacular English, the term “unstable” has a negative connotation. Certainly, no one would want to be described as unstable! This undesirable meaning extends to products of engineering design; we generally want our plants and control systems to be stable. To ensure consistency, we will use a clear and precise definition of

stability, termed *bounded input–bounded output stability*, which can be employed in the design and analysis of process control systems.

A system is **stable** if all output variables are bounded when all input variables are bounded. A system that is not stable is **unstable**.

A variable is *bounded* when it does not increase in magnitude to $\pm\infty$ as time increases. Typical bounded inputs are step changes and sine waves; an example of an unbounded input is a ramp function. Naturally, process output variables do not approach $\pm\infty$ in a chemical plant, but serious consequences occur when these variables *tend toward* $\pm\infty$ and reach large deviations from their normal values. For example, liquids overflow their vessels; closed vessels burst from high pressures; products degrade; and equipment is damaged by excessive temperatures. Thus, substantial incentives exist for maintaining plant variables, with and without control, at stable operating conditions.

As a further clarification, a chemical reactor would be stable according to our definition if a step increase of 1°C in its inlet temperature led to a new steady-state outlet temperature that was 100°C higher. Thus, systems that are very sensitive can be stable as long as they attain a steady state after a step change. The methods in this chapter determine stability strictly as defined here, which is required for good operation but clearly is not alone sufficient to ensure good control performance. Other aspects of achieving acceptable control performance will be addressed in Chapter 13.

10.3 ■ STABILITY OF LINEAR SYSTEMS—A SIMPLE EXAMPLE

Since control system stability is the goal of this chapter, the definition will be reinforced through a process example that shows how the addition of feedback control changes the dynamic response of a linear process. In the next section, the analysis is generalized to any linear system.

EXAMPLE 10.1.

Diameter = 3 m
Height = 3 m

The response of the non-self-regulating level process in Figure 10.1 to a step change in the inlet flow is to be determined for a case with proportional-only control.

The linear models for the process and the controller are

$$A \frac{dL}{dt} = F_{in} - F_{out} \quad (10.1)$$

$$F_{out} = K_c(SP - L) + (F_{out})_s$$

Expressing variables in deviation form, equating the set point and initial steady state (i.e., $L' = L - L_s = L - SP$), and combining into one equation gives

$$A \frac{dL'}{dt} = F'_{in} + K_c L' \quad (10.2)$$

By taking the Laplace transform and rearranging, the transfer function for this

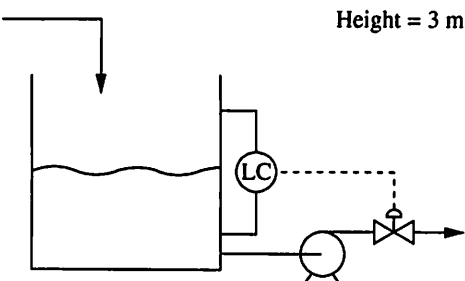


FIGURE 10.1

Level process for Examples 10.1 and 10.3.

system can be derived as

$$\frac{L(s)}{F'_{\text{in}}(s)} = \frac{-1/K_c}{\left(\frac{A}{-K_c}\right)s + 1} \quad (10.3)$$

Solution. Since the system is simple, the following analytical solution to the equations can be derived for a step change in the inlet flow, $F'_{\text{in}}(s) = \Delta F_{\text{in}}/s$.

$$L' = \frac{\Delta F_{\text{in}}}{-K_c} (1 - e^{-t/\tau}) \quad (10.4)$$

with $\tau = A/(-K_c)$. As can be seen, the controller gain affects the time constant of the feedback system. As observed in earlier examples, increasing the magnitude of the controller gain, which gives negative feedback control (which in this case is $K_c < 0$), decreases the time constant as well as reducing the steady-state offset.

Note that for this first-order system the controller gain can be set to a very large magnitude without causing instability. This conclusion can be demonstrated by analyzing the expression for the time constant, which would have to change sign to cause instability. Since the time constant is positive and the analytical solution has a negative exponent for all gains ($K_c < 0$), this idealized system is stable for any negative feedback controller gain. This result is not true for most processes, as will be demonstrated in later examples.

Recall that this analysis is valid only for the ideal, linear level control system described in equations (10.1), which has no sensor or final element dynamics and is perfectly linear. Also, this analysis ensures only that variables do not increase without bound; it does not ensure that the process variables in the real plant will remain within acceptable limits. Applying the final value theorem, the ultimate value of the level after a step change in the inlet flow is

$$\lim_{t \rightarrow \infty} L = \lim_{s \rightarrow 0} sL(s) = \lim_{s \rightarrow 0} s \frac{\frac{\Delta F_{\text{in}}}{(-K_c)s}}{\frac{A}{(-K_c)s} + 1} = \frac{\Delta F_{\text{in}}}{-K_c} \quad (10.5)$$

Substituting the process data into this expression for a $20 \text{ m}^3/\text{h}$ change in flow and a controller gain of $-10 \text{ m}^3/\text{h/m}$ gives a final level deviation of 2 m , which, assuming that the level began in the middle of its range, is half a meter above the top of the tank wall! For this input the plant demonstrates nonlinear behavior by overflowing and is not modelled accurately by equations (10.1) when overflow occurs. Clearly, good control performance requires more than stability; however, stability is one essential component of a well-performing control system.

This example demonstrates that the stability of the level system depends on the sign of the exponential term in the solution and that the feedback controller affects the exponential term. In the next section, the relationship of the exponential term to stability is generalized to address a set of ordinary differential equations of arbitrary order.

10.4 STABILITY ANALYSIS OF LINEAR AND LINEARIZED SYSTEMS

Essentially all chemical processes are nonlinear. Since no general stability analysis of nonlinear systems is available, the *local* stability of the linearized approximation about a steady state is evaluated. The local linear analysis is valid only in

a very small region (theoretically, a differential region) about the linearization conditions. We will assume that a differential region exists about the steady-state operating conditions within which stability can be investigated, and Perlmutter (1972) gives a thorough justification of the linearized analysis, sometimes referred to as *Liapunov's first method*.

Since the control system reduces variability in the controlled variables, the linear stability analysis is often adequate for making the control design and tuning decisions. However, we must recognize that the analysis is valid only at a point and that no rigorous conclusions can be drawn for a finite distance from this point. The successes of the vast majority of process control strategies designed using linear methods attest to the validity of the approach, when applied judiciously.

To develop a general stability analysis for linearized systems, the following n -th-order linear dynamic model with a forcing function $f(t)$ is considered.

$$\frac{d^n Y}{dt^n} + a_1 \frac{d^{n-1} Y}{dt^{n-1}} + \cdots + a_n Y = f(t) \quad (10.6)$$

Note that we often formulate the model as a set of first-order differential equations, which can be combined in the form of equation (10.6) by any of several procedures, such as taking the Laplace transform of the original models and combining algebraically.

The solution to equation (10.6) is composed of two terms: the *particular* solution, which depends on the forcing function, and the *homogeneous* solution, which is independent of the forcing function (Boyce and Diprima, 1986). The forcing functions for process control systems are set point changes and disturbances in process variables such as feed composition, which, since they are bounded, cannot cause instability in an otherwise stable system. Thus, we conclude that the particular solution of a stable system with bounded inputs must be stable. Therefore, the stability analysis concentrates on the homogeneous solution, which determines whether the system is stable, with or without forcing, as long as the inputs are bounded (Willems, 1970).

The Laplace transform of the homogeneous part of equation (10.6), with all initial conditions equal to zero, is

$$(s^n + a_{n-1}s^{n-1} + \cdots + a_1s + a_0)Y(s) = 0 \quad (10.7)$$

As demonstrated in Chapter 4, the solution to equation (10.7) is of the form

$$Y(t) = A_1 e^{\alpha_1 t} + \cdots + (B_1 + B_2 t + \cdots) e^{\alpha_p t} + \cdots + [C_1 \cos(\omega t) + C_2 \sin(\omega t)] e^{\alpha_q t} + \cdots \quad (10.8)$$

where α_i = the i th real distinct root of the characteristic polynomial

α_p = repeated real root of the characteristic polynomial

α_q = real part of complex root of the characteristic polynomial

A, B, C = constants depending on the initial conditions

The stability of the linearized system is entirely determined by the values of the exponents (the α 's). When all of the exponents have negative real parts, the solution cannot increase in an unlimited fashion as time increases. However, if one or more exponents have positive real parts, variables in the system will be unbounded as time increases, and the system will be unstable by our definition. The special case of a zero real part is considered in Example 10.3, where it is shown

that a system with one or more zero real parts is bounded input–bounded output unstable. Thus, a test for stability involves determining all exponential terms and can be summarized in the following principle.

- The *local* stability of a system about a steady-state condition can be determined from a linearized model.
- The linear approximation of the system is bounded input–bounded output stable if all exponents have negative real parts and is unstable if any exponential real part is zero or positive.

The linear approximation is valid only at the point of linearization. If the process operation changes significantly, the stability can be determined for several points with different operating conditions. However, the fact that a system may be stable for many points does not ensure that it is stable for conditions between these stable points. This is sometimes referred to as *pointwise* or *local* stability determination.

EXAMPLE 10.2.

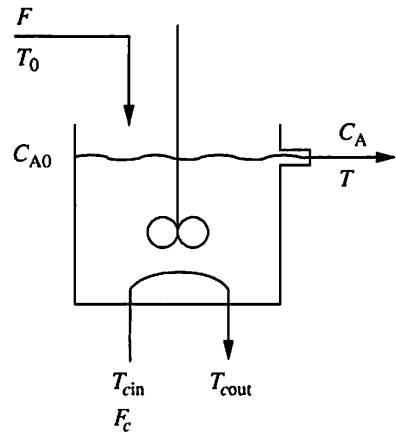
Determine the stability of the variable $T'(t)$ from the following model.

$$\frac{d^2T'}{dt^2} - 1.23 \frac{dT'}{dt} - 1.38T' = 0 \quad (10.9)$$

The exponential terms can be evaluated according to the following procedure.

$$\begin{aligned} (s^2 - 1.23s - 1.38)T'(s) &= 0 \\ s^2 - 1.23s - 1.38 &= 0 \\ s = -0.71 &\quad s = 1.94 \leftarrow \text{unstable!} \\ T'(t) &= A_1 e^{-0.71t} + A_2 e^{1.94t} \end{aligned} \quad (10.10)$$

It is clear that $T'(t)$ is locally unstable about the steady state, because one of the exponential terms has a real part greater than zero. Insight into the cause of instability in a process without feedback control is given in Appendix C, where a chemical reactor is analyzed. (The numerical values for this example are from Case II in Appendix C, Table C.1.)



EXAMPLE 10.3.

The stability of the level process *without* control ($K_c = 0$) shown in Figure 10.1 is to be determined. The vessel size and steady-state flow are the same as in Example 10.1. A material balance on the vessel results in the following model:

$$A \frac{dL(t)}{dt} = F_{in}(t) - F_{out}(t) \quad (10.11)$$

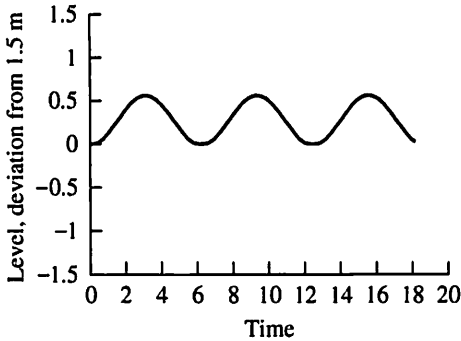
The model can be written in deviation variables and in transfer function form for the case with the outlet flow constant:

$$A \frac{dL'(t)}{dt} = F'_{in}(t) \quad (10.12)$$

$$\frac{L(s)}{F_{in}(s)} = \frac{1}{As} \quad (10.13)$$

The solution to this equation has a real part of the exponential equal to zero. We will assume that the process is initially at steady state and investigate the behavior of the level for two different input flows. First, assume that the flow in varies around its steady-state value according to a sine, $M \sin(\omega t)$, and the system is initially at steady state. The analytical solution for the level is as follows, and the dynamic behavior is shown in Figure 10.2 with $A = 7.1 \text{ m}^2$, $M = 2 \text{ m}^3/\text{mm}$, and $\omega = 1 \text{ rad/min}$.

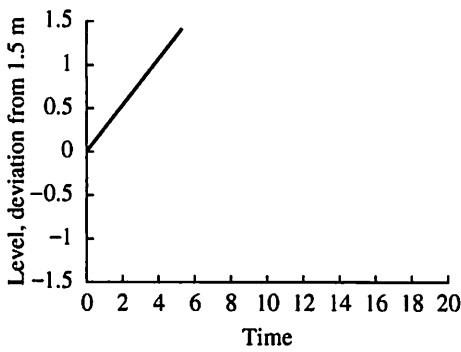
$$L'(t) = \frac{M}{A\omega} [1 - \cos(\omega t)] = 0.282(1 - \cos(t)) \quad (10.14)$$

**FIGURE 10.2**

Response of the level in Example 10.3 to a sine flow disturbance.

For this bounded input function, the output of the linearized system is bounded; therefore, the system is stable in this case. The second case involves a step function in the inlet flow, which increases by $2 \text{ m}^3/\text{h}$ at time = 0. The analytical solution for the level subject to a step change of magnitude M from an initial steady state is as follows, and the dynamic behavior is shown in Figure 10.3.

$$L'(t) = \frac{M}{A} t = 0.282t \quad (10.15)$$

**FIGURE 10.3**

Response of the level in Example 10.3 to a step flow disturbance.

For this bounded input, the output of the linearized model is unbounded (although the true nonlinear level is bounded because the maximum level is reached and the liquid overflows). Thus, the result of the stability analysis indicates a serious deficiency in the level process behavior without control, which should be modified through feedback.

The difference between the behavior of the levels in these two cases is due to the nature of the forcing functions. The sine variation in deviation variables has a zero integral over any multiple of its period; thus, the level increases and decreases but does not accumulate. The step forcing function has a nonzero integral that increases with time, and the level, which integrates the difference between input and output, increases monotonically toward infinity. Since we are interested in general statements on stability that are valid for *all bounded inputs*, we shall consider a system with a zero real part in its exponential to be unstable, because it is unstable for some bounded input functions.

Local stability analysis using linearized models determines stability at the steady state; no rigorous information about behavior a finite deviation from the steady state is obtained.

10.5 □ STABILITY ANALYSIS OF CONTROL SYSTEMS: PRINCIPLES

Again, the local stability of a system will be evaluated by analyzing the linearized model. The analysis method for linear systems can be tailored to feedback control systems by considering the models in transfer function form. The resulting methods will be useful in (1) determining the stability of control designs, (2) selecting tuning constant values, and (3) gaining insight into how process characteristics influence tuning constants and control performance. We begin by considering a general

transfer function for a linear control system in Figure 10.4.

$$\frac{CV(s)}{SP(s)} = \frac{G_p(s)G_v(s)G_c(s)}{1 + G_p(s)G_v(s)G_c(s)G_s(s)} \quad (10.16)$$

$$\frac{CV(s)}{D(s)} = \frac{G_d(s)}{1 + G_p(s)G_v(s)G_c(s)G_s(s)}$$

For the present, we will consider only the disturbance transfer function and will assume that the transfer function can be expressed as a polynomial in s as follows:

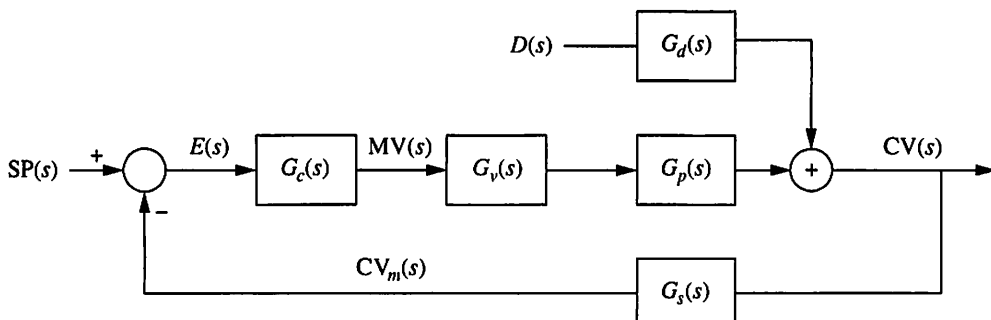
$$(1 + G_p(s)G_v(s)G_c(s)G_s(s)) CV(s) = G_d(s)D(s) \quad (10.17)$$

$$(s^n + a_1s^{n-1} + a_2s^{n-2} + \dots) CV(s) = (s - \beta_1)(s - \beta_2) \dots (s - \beta_m)D(s)$$

The right-hand side (the numerator of the original transfer function) represents the forcing function, which is always bounded because physical input variables cannot take unbounded values, and we assume that the disturbance transfer function, $G_d(s)$, is *stable*.

The essential information on stability is in the left-hand side of equation (10.17), called the *characteristic polynomial*, which is the denominator of the closed-loop transfer function. In the system being considered, Figure 10.4, the characteristic polynomial is $1 + G_p(s)G_v(s)G_c(s)G_s(s)$. Setting the characteristic polynomial to zero produces the *characteristic equation*.

Before continuing, it is important to note that either transfer function in equation (10.16) could be considered, because the characteristic equations of both are identical. Thus, the stability analyses for set point changes and for disturbances yield the same results. Examination of the characteristic equation demonstrates



Transfer Functions

- $G_c(s)$ = Controller
- $G_v(s)$ = Transmission, transducer, and valve
- $G_p(s)$ = Process
- $G_s(s)$ = Sensor, transducer, and transmission
- $G_d(s)$ = Disturbance

Variables

- $CV(s)$ = Controlled variable
- $CV_m(s)$ = Measured value of controlled variable
- $D(s)$ = Disturbance
- $MV(s)$ = Manipulated variable
- $SP(s)$ = Set point

FIGURE 10.4
 Block diagram of a feedback control system.

that the equation contains all elements in the feedback control loop: process, sensors, transmission, final elements, and controller. As we would expect, all of these terms affect stability. The disturbances and set point changes are not in the characteristic equation, because they affect the input forcing; therefore, they do not affect stability. Naturally, the numerator terms affect the dynamic responses and control performance and must be considered in the control performance analysis, although not in this part, which establishes stability.

Continuing the stability analysis, the solution to the homogeneous solution is evaluated to determine stability. For the transfer function, the exponents can be determined by the solution of the following equation resulting from equation (10.17):

$$(s^n + a_1 s^{n-1} + a_2 s^{n-2} + \dots) = 0 \quad (10.18)$$

As before, if any solution of equation (10.18) has a real part greater than or equal to zero, the linearized system is unstable, because the controlled variable increases without limit as time increases. The stability test is summarized as follows:

A linearized closed-loop control system is **locally stable** at the steady-state point if all roots of the characteristic equation have negative real parts. If one or more roots with positive or zero real parts exist, the system is **locally unstable**.

Recall that the roots of the characteristic equation are also referred to as the *poles* of the closed-loop transfer function, e.g., $G_d(s)/[1+G_p(s)G_v(s)G_c(s)G_s(s)]$. This approach to determining stability is applied to two examples to demonstrate typical results.

EXAMPLE 10.4.

The stability of the series chemical reactors shown in Figure 10.5 is to be determined. The reactors are well mixed and isothermal, and the reaction is first-order in component A. The outlet concentration of reactant from the second reactor is controlled with a PI feedback algorithm that manipulates the flow of the reactant, which is very much smaller than the flow of the solvent. The sensor and final element are assumed fast, and process data is as follows.

Process.

$$V = 5 \text{ m}^3 \quad F_s = 5 \text{ m}^3/\text{min} \gg F_A$$

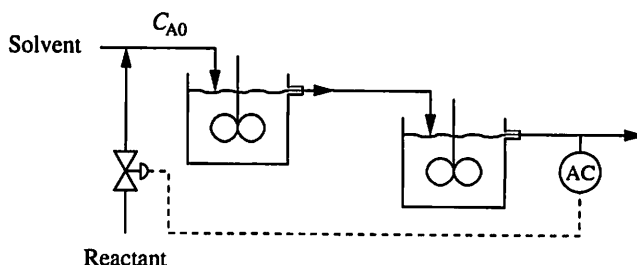


FIGURE 10.5

Series chemical reactors analyzed in Example 10.4.

$$v_s = 50\% \text{ open}$$

$$C_{A0} = 20 \text{ mole/m}^3 \quad k = 1 \text{ min}^{-1}$$

$$C_{A0}(s)/v(s) = K_v = 0.40 \text{ (mole/m}^3\text{)}/(\% \text{ open})$$

PI Controller.

$$K_c = 15(\% \text{ open})/(\text{mole/m}^3)$$

$$T_l = 1.0 \text{ min}$$

Formulation. The process model structure for this system is the same as for Example 3.3, but the data is different and the valve gain is included. The transfer functions for the process and controller are

$$\begin{aligned} G_p(s) &= \frac{K_p}{(\tau s + 1)(\tau s + 1)} \\ G_c(s) &= K_c \left(1 + \frac{1}{T_l s} \right) \end{aligned} \quad (10.19)$$

with

$$\begin{aligned} K_p &= K_v \left(\frac{F}{F + VK} \right)^2 = 0.10 \frac{\text{mole/m}^3}{\%} \\ \tau &= \left(\frac{V}{F + VK} \right) = 0.50 \text{ min} \end{aligned}$$

The individual transfer functions can be combined to give the closed-loop transfer function for a set point change, which includes the characteristic equation.

$$\frac{CV(s)}{SP(s)} = \frac{G_p(s)G_v(s)G_c(s)}{1 + G_p(s)G_v(s)G_c(s)G_s(s)} = \frac{15 \left(1 + \frac{1}{1.0s} \right) \frac{0.10}{(0.5s + 1)^2}}{1 + 15 \left(1 + \frac{1}{s} \right) \left(\frac{0.1}{(0.5s + 1)^2} \right)} \quad (10.20)$$

Characteristic equation.

$$0 = 1 + 15 \left(1 + \frac{1}{s} \right) \left(\frac{0.1}{(0.5s + 1)^2} \right) \quad (10.21)$$

$$0 = 0.25s^3 + 1.0s^2 + 2.5s + 1.5$$

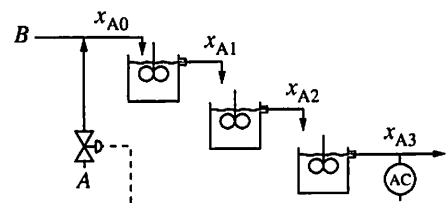
The solution to this cubic equation gives the exponents in the time-domain solution. These values are

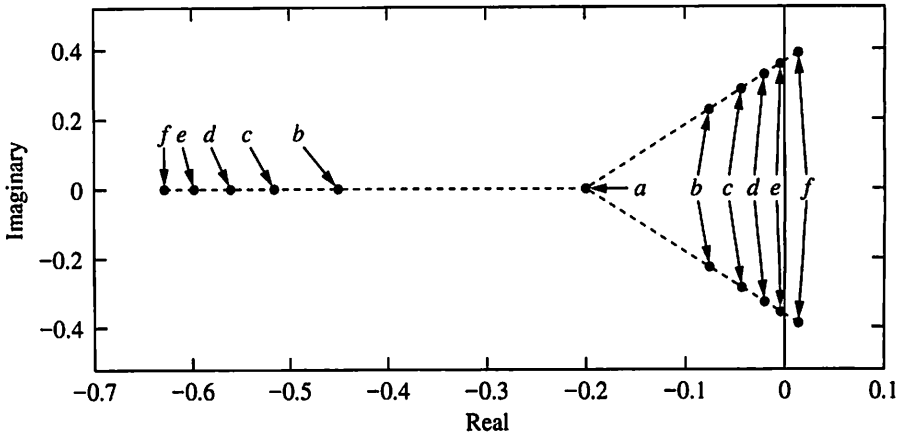
$$\alpha_{1,2} = -1.60 \pm 2.21j \quad \alpha_3 = -0.81$$

Since all roots have negative real parts, this system is stable. Remember, we still do not know how well the closed-loop control system performs, although the complex poles indicate that the system is underdamped and the integral mode indicates that the controlled variable will return to its set point for a steplike disturbance.

EXAMPLE 10.5.

The stability of the three-tank mixing process in Example 7.2 is to be evaluated under feedback control with a proportional-only controller.



**FIGURE 10.6**

Root locus plot for Example 10.5 for controller gain values of (a) 0, (b) 50, (c) 100, (d) 150, (e) 200, and (f) 250.

Assuming that the sensor is fast, $G_s(s) = 1$, the closed-loop transfer function is

$$\frac{CV(s)}{D(s)} = \frac{G_d(s)}{1 + G_p(s)G_v(s)G_c(s)G_s(s)} = \frac{\frac{1}{(5s+1)^3}}{1 + K_c \frac{0.039}{(5s+1)^3}} \quad (10.22)$$

Characteristic equation.

$$125s^3 + 75s^2 + 15s + (1 + 0.039K_c) = 0 \quad (10.23)$$

The solutions to the characteristic equation determine whether the system is stable or unstable. Solutions have been determined for several values of the controller gain (with the proper sign for negative feedback control), and the results are plotted in Figure 10.6. Since the characteristic equation is cubic, three solutions exist. The system without control, $K_c = 0$, is stable, because all roots (i.e., exponential terms) have the same negative real value (-0.2).

As the controller gain is increased from 0 to 250 in increments of 50, the poles approach, and then cross, the imaginary axis. This path can be interpreted as the solution becoming more oscillatory, due to the increasing size of the imaginary parts, and finally becoming unstable, since the exponents have zero and then positive real parts. Based on this analysis, the three-tank mixing process is found to be (barely) stable (and periodic) for $K_c < 200$ and unstable for $K_c > 250$; further study shows that the stability limit is about $K_c = 208$. The control performance would be clearly unacceptable when the system is unstable, but again, we do not yet know for what range of controller gain the control performance is acceptable.

The results of Example 10.5 can be generalized to establish relationships between locations of roots of the characteristic equation (poles of the closed-loop transfer function). In addition, features of dynamic responses can be inferred from the poles if a constant transfer function numerator is assumed. These generalizations are sketched in Figure 10.7, which shows the nature of the dynamic responses for various pole locations. Clearly, the numerical values of the poles (or equiva-

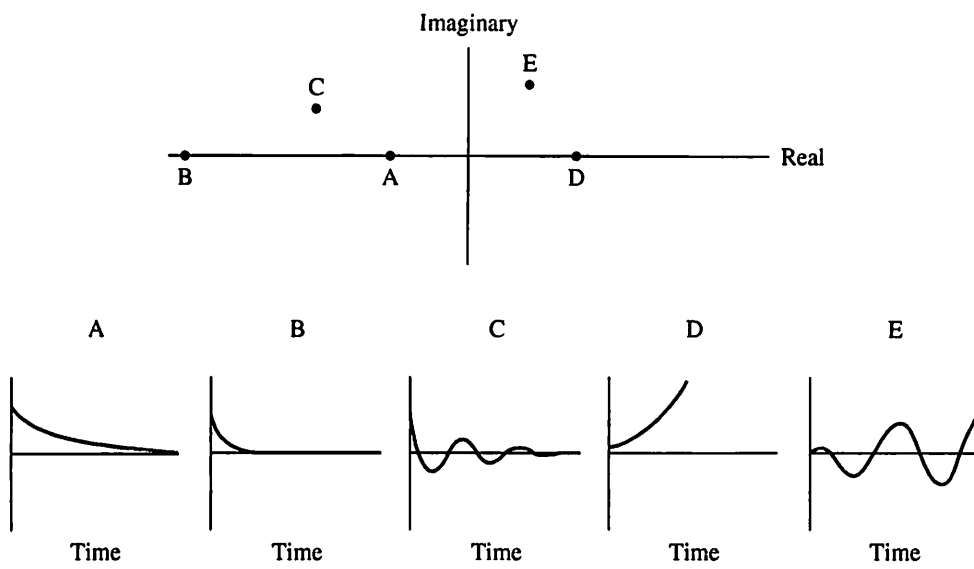


FIGURE 10.7

Examples of the relationship between the locations of the exponential terms and the dynamic behavior.

lently, their location in the complex plane) are very important for the dynamic response of a closed-loop system.

The method of plotting the roots of the characteristic equation as a function of the controller tuning constant(s) is termed *root locus* analysis and has been used for decades. Note that a root-solving computer program is required to facilitate the construction of the plots. We will use another stability analysis method in further studies, but we directly calculated the poles of the closed-loop transfer function here because of the excellent visual display of the effect of the tuning constants on the exponential terms and therefore on stability. In summary, for a linearized model (which determines local properties):

- Application of the general stability analysis method to feedback control systems demonstrates that the roots of the characteristic equation determine the stability of the system.
- When the characteristic equation is a polynomial, a straightforward manner of determining the stability is to calculate the roots of the characteristic equation.
- If all roots have negative real parts, the system is bounded input–bounded output stable; if any root has a positive or zero real part, the system is unstable.

10.6 ■ STABILITY ANALYSIS OF CONTROL SYSTEMS: THE BODE METHOD

The method presented in the previous section presents the principles of stability analysis of transfer functions and provides a vivid picture of the effects of controller tuning on the stability of control systems. However, we would like to have a method for analyzing control systems that

1. Involves simple calculations
2. Addresses most processes of interest
3. Gives information on the *relative stability* of the system (i.e., how much a parameter must change to change the stability of the system)
4. Yields insight into how various process and controller characteristics affect tuning and control performance

The most commonly used stability analysis methods are summarized in Table 10.1. Since many plants in the process industries have dead time, the methods that require polynomial transfer functions (root locus and Routh) will not be considered further. Of the two remaining, the Nyquist method is the most general. However, in spite of a few limitations, the Bode method of stability analysis is selected for emphasis in this book, because it involves simple calculations and, more importantly in the age of computers, gives more easily understood insights into the effect of process and controller elements on the stability of closed-loop systems.

The basis of the Bode method is first explained with reference to the system in Figure 10.8a and b; then, a simple calculation procedure is presented with several worked examples. Suppose that a sine wave is introduced into the set point with the loop maintained open as in Figure 10.8a. Because the system is linear, all variables oscillate in a sinusoidal manner. After some time, the system attains a “steady state,” a standing wave in which the amplitudes do not change. The sine frequency can be selected so that the output signal, $CV(t)$, lags the input signal, $SP(t)$, by 180° . Note that the relative amplitudes of the various signals in Figure 10.8a would normally be different but are shown to be equal here because the process and controller transfer functions have not yet been specified.

After steady state has been attained, the set point is changed to a constant value and the loop is closed, as shown in Figure 10.8b. Since this is a closed-loop system, the sine affects the process output, which is fed back via the error signal to the process input. For the frequency selected with a phase difference of 180° , the returning signal *reinforces* the previous error signal because of the negative sign of the comparator.

TABLE 10.1
Summary of stability analysis methods

Method	Plant model	Stability results	Results display
Root locus (Franklin et al., 1991)	Polynomial in s	Relative	Graphical
Routh (Willems, 1970)	Polynomial in s	Yes or no	Tabular
Bode	(1) Open loop-stable (2) Monotonic decreasing amplitude ratio (AR) and phase angle (ϕ) as frequency increases	Relative	Graphical
Nyquist (Dorf, 1986)	Linear	Relative	Graphical

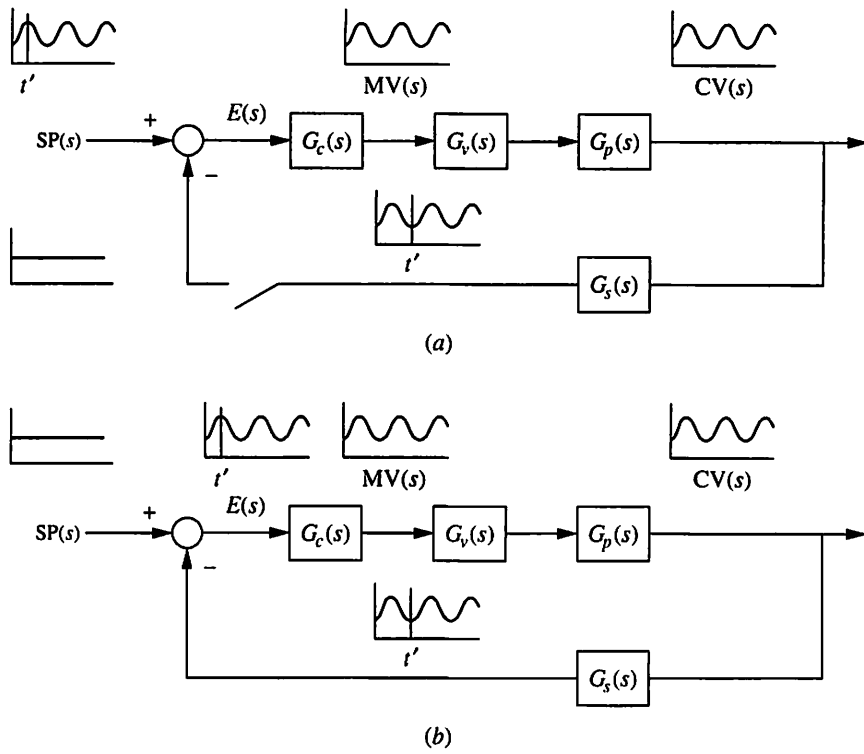


FIGURE 10.8

Bode stability analysis: (a) behavior of open-loop system with sine forcing; (b) behavior of system after the forcing is stopped and the loop is closed.

A key factor that determines the behavior of this closed-loop system is the amplification as the sine wave travels around the control loop once. If the signal decreases in magnitude every pass, it will ultimately reduce to zero, and the system is stable. If the signal increases in amplitude every pass, the wave will grow without limit and the system is unstable. This analysis leads to the Bode stability criterion. Two important factors need to be emphasized. First, the analysis is performed at the frequency at which the feedback signal lags the input signal by 180° ; this is termed the *critical* or *crossover* frequency. Naturally, the critical frequency depends on all of the dynamic elements in the closed-loop system. Second, for the amplitude of the wave to increase, the *gain* of the elements in the loop must be greater than 1. This gain depends on the amplitude ratios of the process, instrument, and controller elements in the loop *at the critical frequency*. The result is the Bode stability criterion for linear systems, which gives local results for a nonlinear system.

The Bode stability criterion states that a closed-loop linear system is stable when its amplitude ratio is less than 1 at its critical frequency. The system is unstable if its amplitude ratio is greater than 1 at its critical frequency.

From this analysis, it is clear that a system with an amplitude ratio of exactly 1.0 would be at the stability limit, with a slight increase or decrease resulting in

instability or stability, respectively. Because of small inaccuracies in modelling and nonlinearities in processes, no real process can be maintained at its stability limit.

Note that the Bode method considers all elements in the feedback loop: process, sensors, transmission, controller, and final element. Naturally, some of these may contribute negligible dynamics and can be lumped into a smaller number of transfer functions. By convention, the transfer function used in the Bode analysis is termed the *open-loop* transfer function and is represented by the symbol $G_{OL}(s)$.

$$G_{OL}(s) = G_p(s)G_v(s)G_c(s)G_s(s) \quad (10.24)$$

Before the Bode method is discussed further, limitations are pointed out. The Bode method *cannot* be applied to a few systems in which $G_{OL}(s)$ has particular features:

1. Unstable without control
2. Nonmonotonic phase angles or amplitude ratios at frequencies higher than the first crossing of -180°

The Bode method is not appropriate for these systems because

1. The experiment in Figure 10.8 cannot be performed for an unstable process.
2. Nonmonotonic behavior in the Bode diagram of $G_{OL}(s)$ could lead to a higher harmonic of the critical frequency for which the magnitude is greater than 1.0.

For processes with these features, the Nyquist stability analysis is recommended (Dorf, 1986).

The amplitude ratio can be determined through analytical relationships introduced in Chapter 4. The important relationships are summarized below for a general transfer function; these were applied to process transfer functions in Chapter 4 and will be extended here to $G_{OL}(s)$. As a brief summary of results in Chapter 4,

1. The frequency response relates the long-time output response to input sine forcing of the system.
2. The frequency response of a linear system can be easily calculated from any stable transfer function, $G(s)$, as $G(j\omega)$.
3. The amplitude ratio is the ratio of the output over the input sine magnitudes and can be calculated as

$$AR = |G(j\omega)| = \sqrt{(\text{Re}[G(j\omega)])^2 + (\text{Im}[G(j\omega)])^2} \quad (10.25)$$

4. The phase angle gives the amount that the output sine lags the input sine and can be calculated as

$$\phi = \angle G(j\omega) = \tan^{-1} \left(\frac{\text{Im}[G(j\omega)]}{\text{Re}[G(j\omega)]} \right) \quad (10.26)$$

Another important simplification provides a way for the frequency response of a series of transfer functions to be calculated from the individual frequency

responses. First, each individual transfer function can be represented in polar form by

$$G_i(j\omega) = |G_i(j\omega)| e^{-\phi_i j} \quad (10.27)$$

The series transfer function can then be expressed as

$$G(j\omega) = \prod_{i=1}^n G_i(j\omega) = \left(\prod_{j=1}^n |G_i(j\omega)| \right) \exp \left(- \sum_{i=1}^n \phi_i j \right) = AR e^{-\Phi j} \quad (10.28)$$

with

$$AR = \prod_{i=1}^n |G_i(j\omega)| \quad \Phi = \sum_{i=1}^n \phi_i$$

These are especially useful relationships, because the individual transfer functions used in the Bode method, $G_{OL}(s)$, are often in series as shown in Figure 10.4 and equation (10.24).

In addition to the simplifications in the calculation, the frequency response of a transfer function can be presented in a clear graphical manner using Bode plots. These plots, introduced in Chapter 4, present the amplitude ratio and the phase angle as a function of the frequency. The log scales are used to cover larger ranges of variable values with reasonable accuracy. The reason for the inclusion of the phase angle plot was not obvious in Chapter 4 but becomes apparent when stability of feedback systems is evaluated, as the next few examples demonstrate.

The frequency response calculations used in the remainder of this chapter involve algebraic manipulations to solve for the amplitude ratio, $|G_{OL}(j\omega)|$, and phase angle, $\angle G_{OL}(j\omega)$, from the transfer function by setting $s = j\omega$. Alternatively, these terms can be evaluated directly using basic computer functions; for example, the following pseudo-code can be used in MATLAB™ to evaluate the amplitude ratio and phase angle of a first-order-with-dead-time transfer function at a specified frequency:

```
Kp = 2.0;
theta = 5.0;
taup = 5.0;
j = sqrt(-1);
omega = 0.20;
Gp = Kp*exp(-theta*omega*j)/(taup*omega*j + 1); % define the complex variable
AR = abs(Gp); % define the value of frequency in rad/time
Phase = angle(Gp); % evaluate Gp(jw), a complex variable
Phase = phase * 180/pi; % absolute value gives the magnitude
% angle gives phase angle in rad
% to obtain degrees, multiply by 180/pi
```

Expressions are provided in Table 10.2 for the amplitude ratio and phase angle of some simple, commonly used transfer functions. Computer calculations demonstrated above can be used for any transfer functions, including those too complex to reduce algebraically.

Therefore, the reader is advised to concentrate on the principles introduced and applications demonstrated in this chapter, with the assurance that no practical limit exists to easily calculating the information needed for stability analysis.

TABLE 10.2

Summary of amplitude ratios and phase angles for common transfer functions (ω is in rad/time, n is a positive integer)

Transfer function	Amplitude ratio*	Phase angle (°)*
K	K	0
$\frac{K}{\tau s + 1}$	$\frac{K}{\sqrt{\tau^2 \omega^2 + 1}}$	$\tan^{-1}(-\omega\tau)$
$\frac{K}{\tau^s s^2 + 2\tau\xi s + 1}$	$\frac{K}{\sqrt{(1 - \tau^2 \omega^2)^2 + (2\tau\omega\xi)^2}}$	$\tan^{-1}\left(\frac{-2\tau\omega\xi}{1 - \tau^2 \omega^2}\right)$
$\frac{K}{(\tau s + 1)^n}$	$K \left(\frac{1}{\sqrt{\tau^2 \omega^2 + 1}}\right)^n$	$n \tan^{-1}(-\omega\tau)$
$e^{-\theta s}$	1	$-\theta\omega\left(\frac{360}{2\pi}\right)$
$\frac{1}{As}$	$\frac{1}{A\omega}$	-90
$K_c \left(1 + \frac{1}{T_I s}\right)$	$K_c \sqrt{1 + \frac{1}{\omega^2 T_I^2}}$	$\tan^{-1}\left(\frac{-1}{\omega T_I}\right)$
$K_c(1 + \tau_d s)$	$K_c \sqrt{1 + (T_d\omega)^2}$	$\tan^{-1}(T_d\omega)$
$K_c \left(1 + \frac{1}{T_I s} + T_d s\right)$	$K_c \sqrt{1 + \left(T_d\omega - \frac{1}{T_I\omega}\right)^2}$	$\tan^{-1}\left(T_d\omega - \frac{1}{T_I\omega}\right)$

*For the gain > 0 .

EXAMPLE 10.6.

The single-tank mixing process with proportional control shown in Figure 10.9 is considered. This process is the same as the three-tank mixer in Example 7.2 with the last two tanks removed. The process transfer function, which includes an ideal sensor and fast final element dynamics, is given as

$$G_c(s) = K_c \quad G_p(s)G_v(s)G_s(s) = \frac{0.039}{5s + 1} \quad (10.29)$$

with time in minutes. Note that the process is stable without control, since it has one pole at $(-0.2, 0)$ in the real-imaginary plane, so that it satisfies the criteria in Table 10.1 for the Bode method. The stability is to be determined by the Bode method.

First, $G_{OL}(s)$ must be determined. This is the product of the valve, process, sensor, and controller transfer functions; $G_{OL}(s)$ with proportional-only control can be written as

$$G_{OL}(s) = \frac{0.039 K_c}{5s + 1} \quad (10.30)$$

FIGURE 10.9

Mixing process analyzed in Example 10.6.

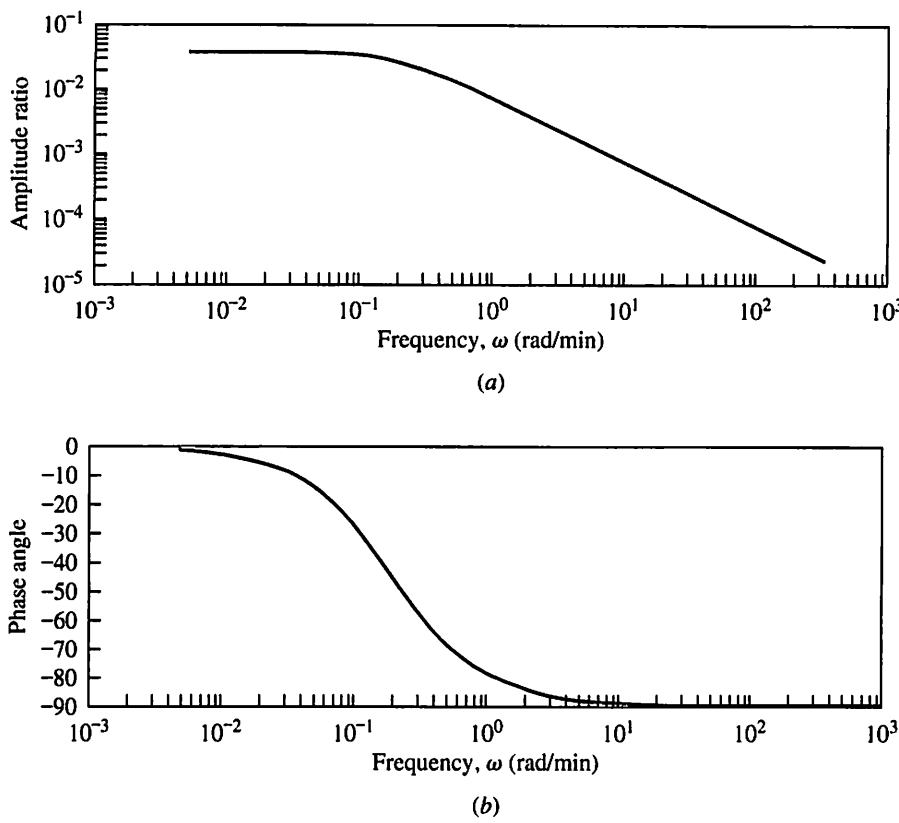


FIGURE 10.10

Bode plot for the $G_{OL}(j\omega)$ in Example 10.6, with $K_c = 1.0$.

The magnitude and phase angle of $G_{OL}(s)$ can be calculated from $G_{OL}(j\omega)$:

$$\begin{aligned}
 AR &= |G_{OL}(j\omega)| \\
 &= \left| (0.039K_c) \left(\frac{1}{1+5j\omega} \right) \left(\frac{1-5j\omega}{1-5j\omega} \right) \right| \\
 &= \frac{(0.039K_c)}{\sqrt{1+25\omega^2}} \\
 \Phi &= \angle G_{OL}(j\omega) = \angle (0.039K_c) + \angle \frac{1}{5s+1} \\
 &= \tan^{-1}(-5\omega)
 \end{aligned} \tag{10.31}$$

These expressions are presented in Bode plots in Figure 10.10 for $K_c = 1$. Since the phase angle for this first-order system does not decrease below -90° for any controller gain, the phase angle never reaches -180° , and the feedback signal cannot reinforce oscillations in the control loop. As a result, this *idealized* control system is stable for all negative feedback proportional-only controller gains ($K_c > 0$ in this case). As the next example illustrates, nearly every realistic system can be made unstable with improper feedback control.

EXAMPLE 10.7.

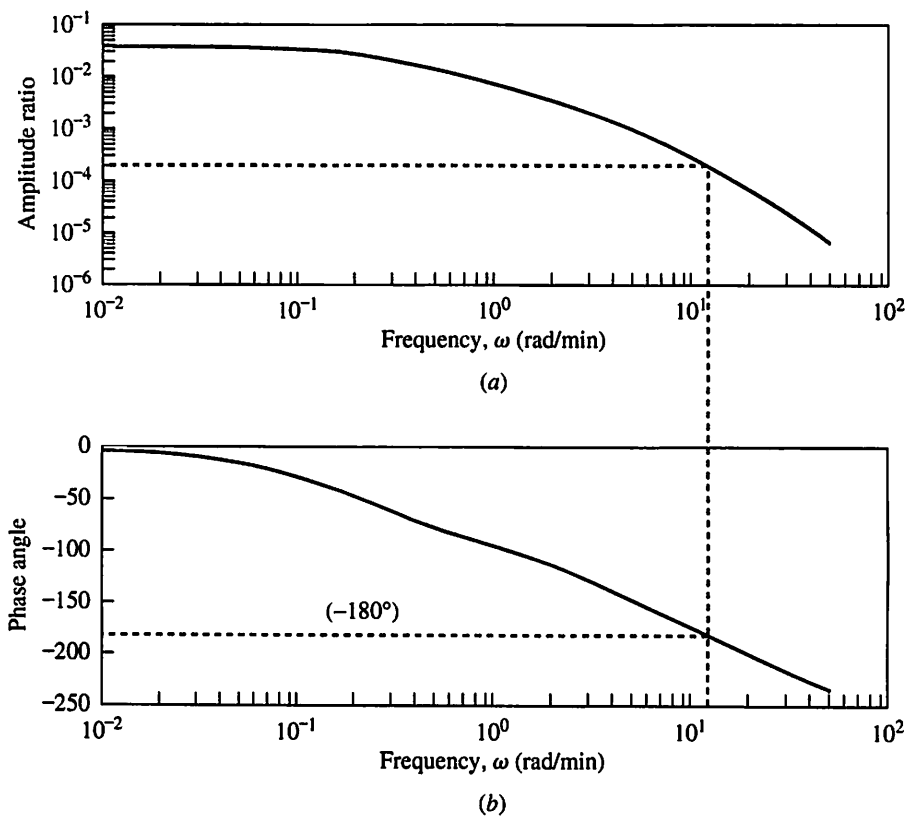
The mixing process and proportional controller in Figure 10.9 and Example 10.6 are considered here, with the modification that the valve and sensor dynamics are more realistically modelled according to the following first-order transfer functions with short time constants:

$$G_c(s) = K_c \quad G_p(s) = \frac{0.039}{5s + 1} \quad G_v(s) = \frac{1}{0.033s + 1} \quad G_s(s) = \frac{1}{0.25s + 1} \quad (10.32)$$

Equations (10.28) can be used to determine the amplitude ratio and phase angle for this series system, and the results are

$$\begin{aligned} G_{OL}(s) &= (0.039K_c) \frac{1}{1+5s} \frac{1}{1+0.25s} \frac{1}{1+0.033s} \\ |G_{OL}(j\omega)| &= \frac{0.039K_c}{\sqrt{1+25\omega^2}} \frac{1}{\sqrt{1+0.0625\omega^2}} \frac{1}{\sqrt{1+0.0011\omega^2}} \\ \angle G_{OL}(j\omega) &= \tan^{-1}(-5\omega) + \tan^{-1}(-0.25\omega) + \tan^{-1}(-0.033\omega) + \angle(0.039K_c) \end{aligned} \quad (10.33)$$

The amplitude ratio and phase angle are plotted in Figure 10.11 for a controller gain of 1.0. Because of the added dynamic elements in $G_{OL}(s)$, the phase angle

**FIGURE 10.11**

Bode plot of $G_{OL}(j\omega)$ for the system in Example 10.7 with $K_c = 1.0$.

exceeds -180° . At the critical frequency (11.6 rad/min), the following values for the amplitude ratio are determined:

$K_c = 1.0$	$ G_{OL}(j\omega_c) = 0.0002 < 1.0$	Stable
$K_c = 500$	$ G_{OL}(j\omega_c) = 0.10 < 1.0$	Stable
$K_c = 6000$	$ G_{OL}(j\omega_c) = 1.2 > 1.0$	Unstable

As can be seen by applying the Bode stability criterion, the system is stable for controller gain values of 1.0 and 500 because the amplitude ratios at the critical frequencies are less than 1.0, and the system is unstable for a controller gain of 6000, which has an amplitude ratio greater than 1.0 at the critical frequency.

Two important lessons have been learned from the last examples. The first lesson is that in theory, a stable transfer function $G_{OL}(s)$ that is first- or second-order cannot be made unstable with proportional-only feedback control, because its phase angle is never less than -180° . The second lesson demonstrates that all real systems have additional dynamic elements in the control loop (e.g., valve, sensor, transmission) that contribute additional phase lag and result in a phase angle less than -180° , albeit at a very high frequency.

Thus, essentially all real process control systems can be made unstable simply by increasing the magnitude of the feedback controller gain.

EXAMPLE 10.8.

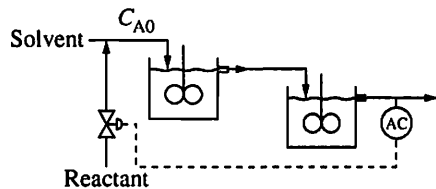
The chemical reactor process and control system in Example 10.4 are changed slightly. In this case, a transportation delay of 1 min exists between the mixing point and the first stirred-tank reactor, with no reaction in the transport delay. Therefore, the process transfer function is modified to include the dead time. A proportional-integral controller is proposed to control this process with the same tuning as Example 10.4; $K_c = 15$ and $T_I = 1$. Determine whether this system is stable.

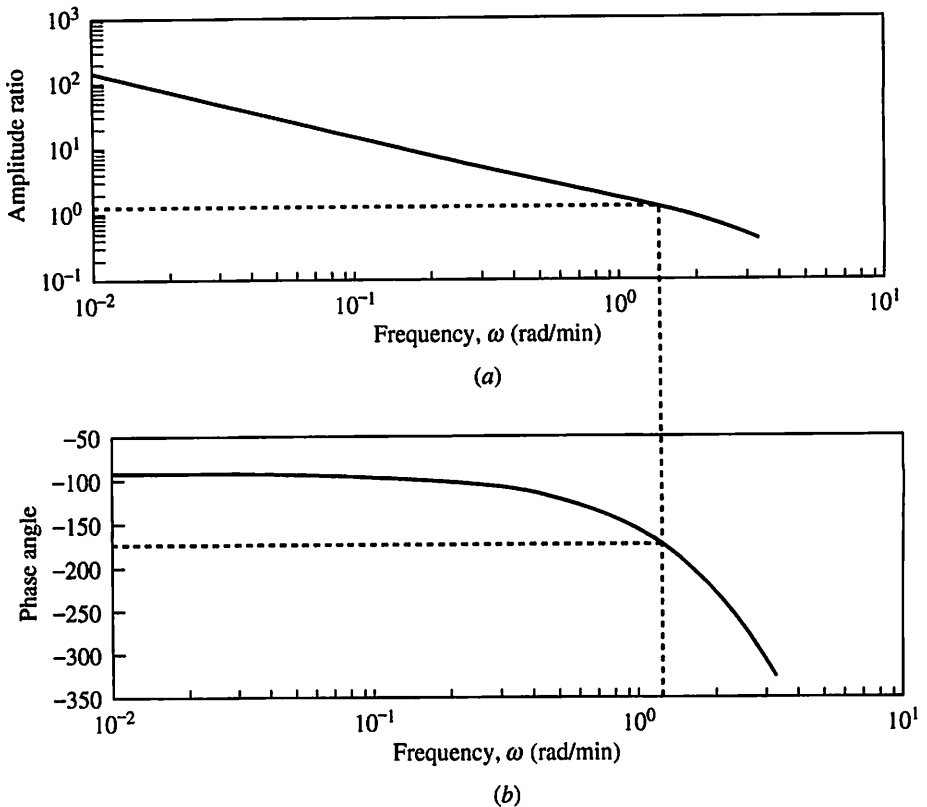
The Bode method can be applied to this example with the new aspect that dead time exists in the process. The first task is to determine $G_{OL}(s)$. As explained above, this transfer function contains all elements in the feedback loop; therefore, $G_{OL}(s)$ is

$$G_{OL}(s) = 15 \left(1 + \frac{1}{s} \right) \frac{0.10e^{-s}}{(0.50s + 1)^2} \quad (10.34)$$

The amplitude ratio and phase angle for each element can be combined to give the amplitude ratio and phase angle of $G_{OL}(j\omega)$.

$$\begin{aligned} AR &= \left| 15 \left(1 + \frac{1}{j\omega} \right) \right| \left| \frac{0.10}{(0.50j\omega + 1)^2} \right| |e^{-j\omega}| \\ &= 15 \sqrt{1 + \frac{1}{\omega^2}} \frac{0.10}{(1 + 0.25\omega^2)} (1.0) \end{aligned}$$



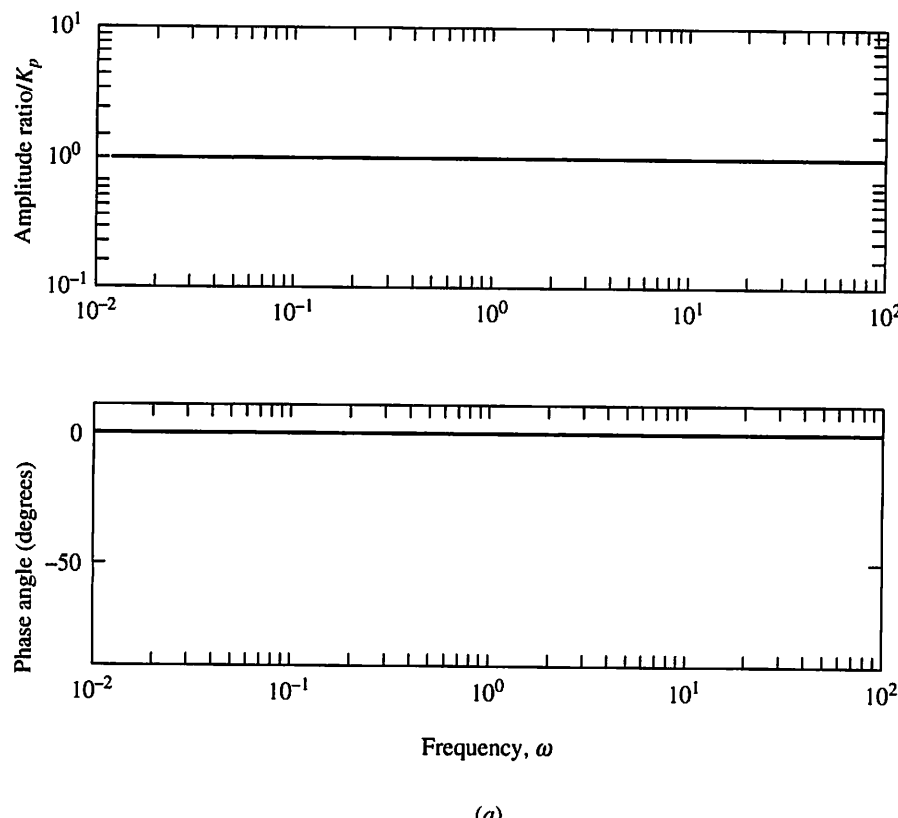
**FIGURE 10.12**

Bode plot of $G_{OL}(j\omega)$ for Example 10.8.

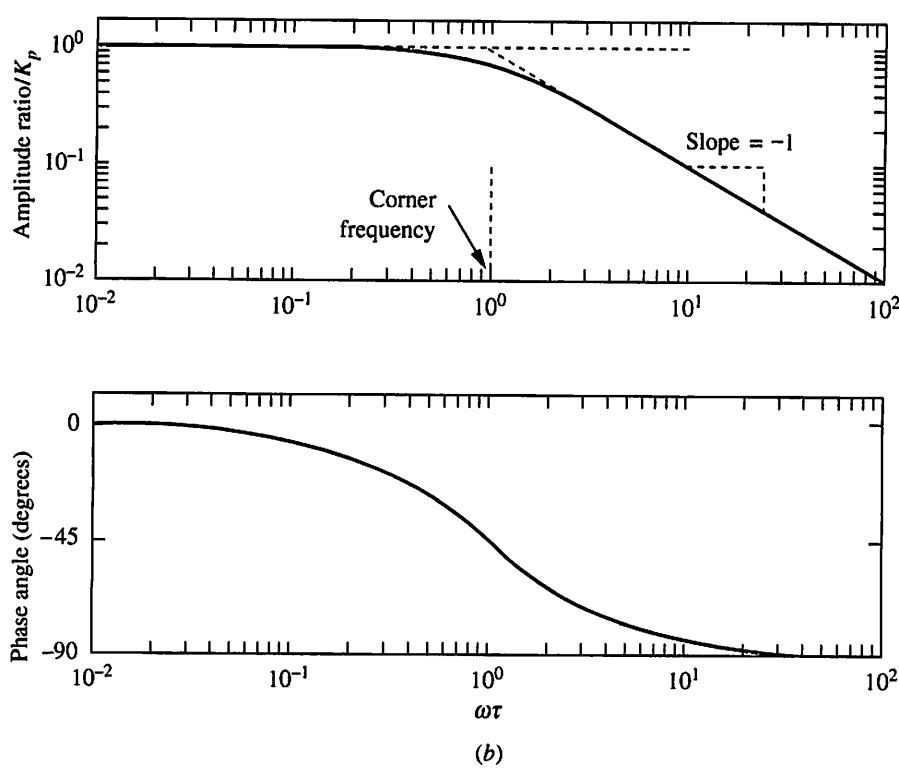
$$\begin{aligned}\Phi &= \angle 15 + \angle \left(1 + \frac{1}{j\omega}\right) + \angle \left(\frac{0.10}{(0.50j\omega + 1)^2}\right) + \angle e^{-j\omega} \\ &= \tan^{-1}(-1/\omega) + 2\tan^{-1}(-0.5\omega) - 1.0\omega \frac{360}{2\pi}\end{aligned}$$

These terms are plotted in Figure 10.12. Since the amplitude ratio is greater than 1 (1.32) at the critical frequency of 1.31 rad/min, the system is unstable. Note that the dead time introduced additional phase lag in the feedback system and caused the system to become unstable. This result agrees with our qualitative understanding that processes with dead time are more difficult to control via feedback. Stable control could be obtained by adjusting the tuning constant values.

The preceding examples have demonstrated interesting results. To expand on these experiences, it would be valuable to understand the contributions of commonly occurring process models and controller modes to the stability of a feedback control system. Also, it would be useful, when performing calculations, to have analytical and sample graphical frequency responses for these common elements. Both of these goals are satisfied by the analytical expressions and Bode plots presented to complete this section. The plots for the key process components—gain, first-order, second-order, pure integrator, and dead time—are presented in Figure 10.13a through e; these were developed from the transfer functions and expressions



(a)

**FIGURE 10.13**

Generalized Bode plots: (a) gain; (b) first-order system.

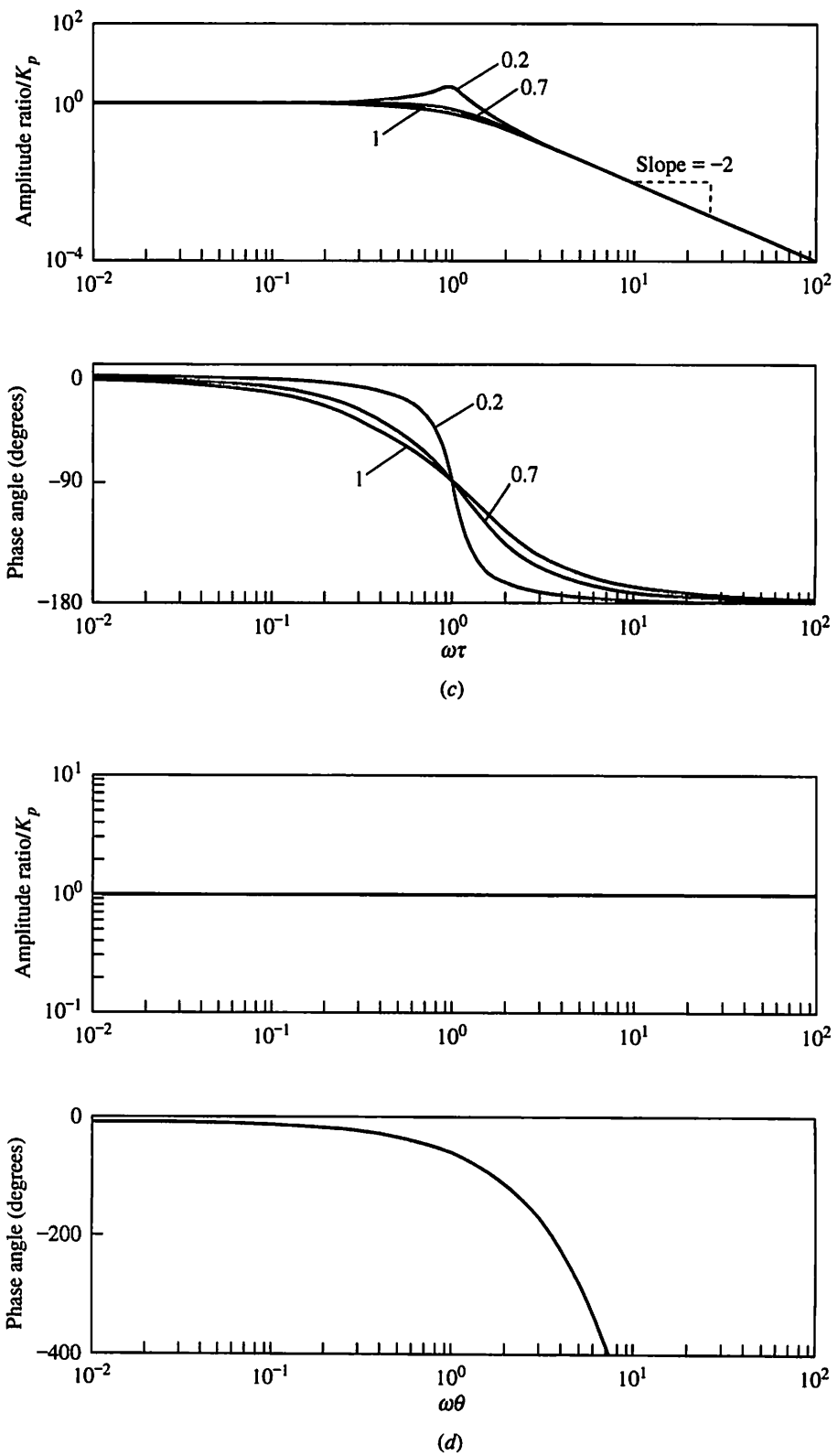
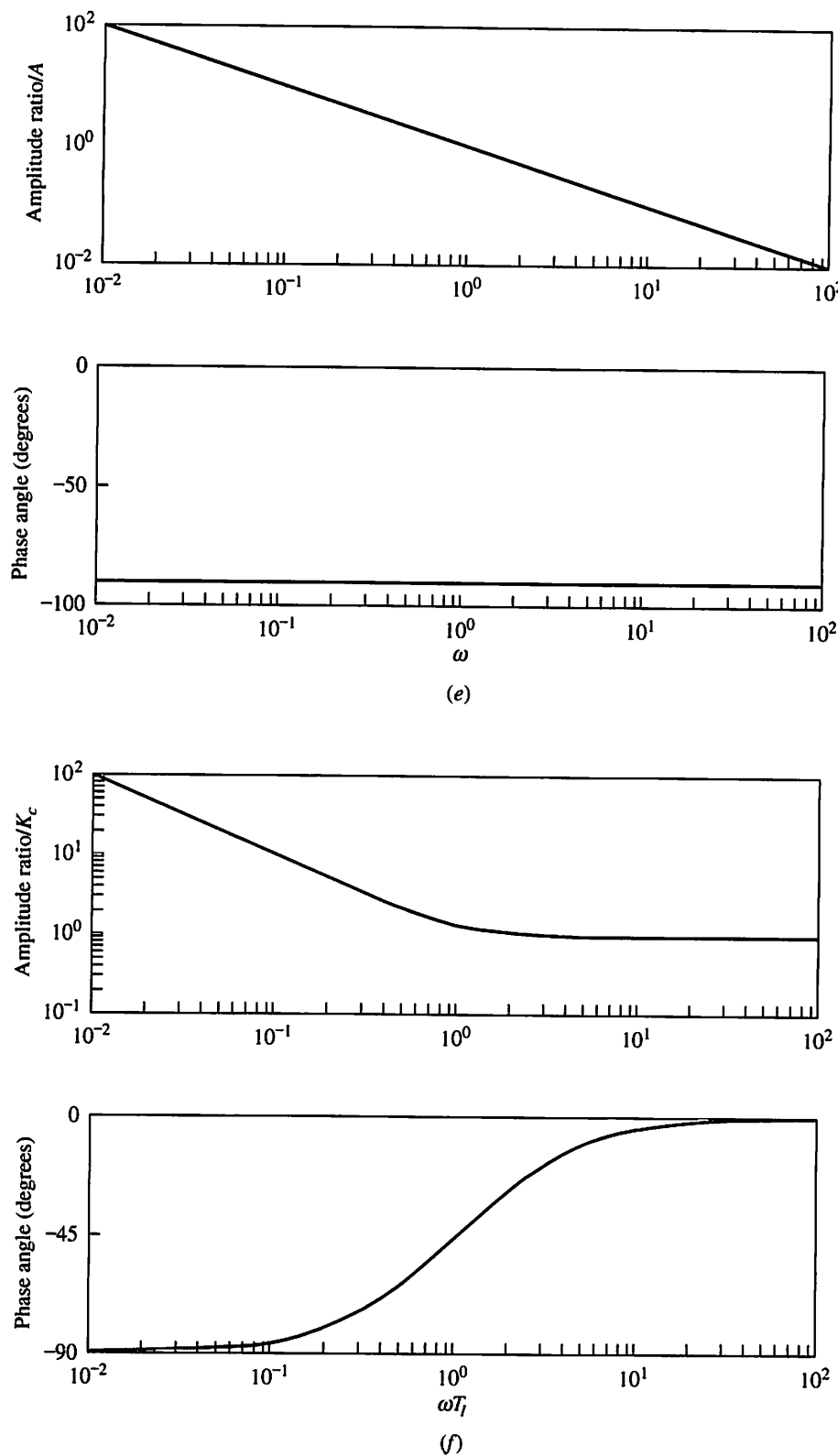


FIGURE 10.13 Con't.

Generalized Bode plots: (c) second-order system (the parameter is the damping coefficient ξ); (d) dead time.


FIGURE 10.13 Con't.

Generalized Bode plots: (e) integrator; (f) proportional-integral controller.

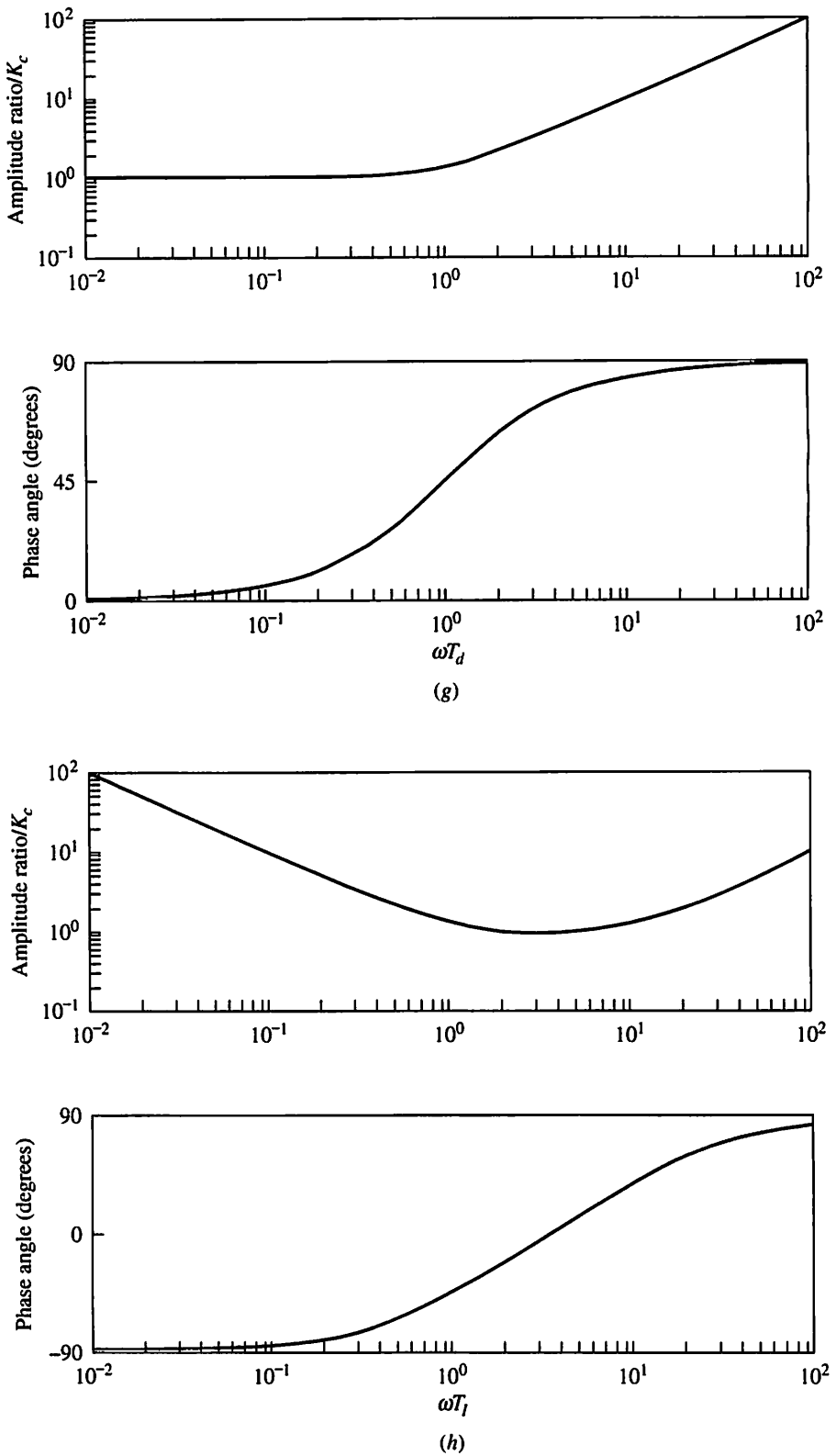


FIGURE 10.13 Con't.

Generalized Bode plots: (g) proportional-derivative controller; (h) proportional-integral-derivative controller for which the derivative time is one-tenth of the integral time.

for amplitude ratio and phase angle in Table 10.2. The plots for the PI, PD, and PID controllers are presented in Figure 10.13*f* through *h* and were also developed from the analytical expressions in Table 10.2. Note that these plots are presented in dimensionless parameters, so that they can be used to determine the frequency responses quickly for a system conforming to one of the general models. The tables and generalized figures are valid for the frequency responses of transfer functions with positive gains. When the gain is negative, (1) the amplitude ratio should be determined using the *absolute value* of the gain, $|K|$, and (2) the phase angle is *smaller by 180°* (or π radians), i.e., $(\angle G(j\omega))_{K<0} = (\angle G(j\omega))_{K>0} - 180^\circ$.

As an example of the preparation of the dimensionless plots, the expressions for the amplitude ratio and phase angle for a first-order system are given in Table 10.2 and repeated here:

$$\begin{aligned} AR &= \frac{K_p}{\sqrt{\omega^2\tau^2 + 1}} & \frac{AR}{K_p} &= \frac{1}{\sqrt{\omega^2\tau^2 + 1}} \\ \phi &= \tan^{-1}(-\omega\tau) \end{aligned} \quad (10.36)$$

Noting that the two variables ω and τ always appear as a product, they can be combined into one variable, $\omega\tau$, and the Bode plots expressed as a function of this single variable. Also, the amplitude ratio can be normalized by dividing by the process gain K_p . Similar manipulations are possible for the transfer functions of the other building blocks.

EXAMPLE 10.9.

Determine the amplitude ratio and phase angle of the following transfer function at a frequency of 0.40 rad/min:

$$G(s) = \frac{0.039}{(1+5s)^2} \quad (10.37)$$

The first step is to calculate the parameters in the generalized Figure 10.13*c*. The results can be calculated as follows:

$$\tau^2 = 25 \quad \tau = 5.0 \quad \xi = \frac{10}{2\tau} = 1.0 \quad (10.38)$$

From the generalized charts, $AR/K_p = 0.2$; $AR = 0.2(0.039) = 0.0078$; and $\phi = -125^\circ$. The same answers can be determined by using the equations in Table 10.2.

The Bode plot of any $G_{OL}(j\omega)$ for a system consisting of a series of common elements can be easily prepared by using the expressions for these individual elements and equation (10.28). The usefulness of the general plots is not primarily in simplifying the calculations, because the calculations are not difficult by hand and computer programs are available to automate the calculations and plot the results. The real importance is in highlighting the contributions of various components to the stability of a feedback system. For example, note that an element in the feedback path that has a large phase angle contributes to lowering the critical frequency. Since most process models have amplitudes that decrease with increasing frequency, a lower critical frequency yields a higher amplitude ratio for $G_{OL}(j\omega)$. Since a lower amplitude ratio is desired to maintain the amplitude ratio below 1.0

for stability, elements with the larger phase angle tend to destabilize a feedback control system. Some of the key features of the most important transfer functions are summarized in Table 10.3. The readers are encouraged to compare the entries in the table with the Bode figures so that they understand the major contributions of each transfer function.

Before we move on to controller tuning, a word of caution regarding terminology is provided. The common term for the expression in equation (10.24), $G_{OL}(s)$, is the open-loop transfer function; hence, the subscript OL. The term refers to Figure 10.8, where the feedback loop was temporarily opened. Unfortunately, the term *open-loop* is also used for the response of a process to an input change without control. In this second case, the transfer function being considered is either the process transfer function $G_p(s)$ or the disturbance transfer function $G_d(s)$, depending on which input-output relationship is being considered. To avoid misinterpretation, it is best to relate the subscript OL to Figure 10.8 and to recognize that $G_{OL}(s)$ contains all elements in the feedback loop, *including the controller*. The conventional terminology, although not as clear as desired, is used in this book to prevent confusion when consulting other references.

TABLE 10.3
Summary of key features of process transfer function frequency responses

Transfer function	Amplitude ratio, AR	Phase angle, ϕ	Key feature
Gain, K	Constant	0	
First-order, $1/(\tau s + 1)$	Monotonically decreases with increasing frequency, limiting slope = -1	0 to -90°	At corner frequency ($\omega = 1/\tau$), AR = 0.707, and $\phi = -45^\circ$
Second-order, $1/(\tau^2 s^2 + 2\xi\tau s + 1)$	(1) Shape depends on the damping ratio, can be nonmonotonic (2) Limiting slope = -2	0 to -180°	(1) AR is not monotonic for small damping coefficients (2) Key frequency is $\omega = 1/\tau$
n th order from n first order in series, $1/(\tau s + 1)^n$	Monotonically decreases with increasing frequency, limiting slope = $-n$	0 to $(-90)n^\circ$	
Dead time, $e^{-\theta s}$	1.0	0 to $-\infty$	At $\omega = 1/\theta$, $\phi = -57.3^\circ$ and decreases rapidly as ω increases
Integrator, $1/A s$	Straight line with a slope of -1 from $-\infty$ to $+\infty$ through ($\omega = 1$, AR = 1)	-90°	At $\omega = 1/A$, AR = 1

Notes:

1. All slopes refer to the Bode diagram ($\Delta \log(\text{AR})/\Delta \log(\omega)$).
2. The phase angles for all transfer functions in this table decrease monotonically as frequency increases.
3. Phase angle values for the case with positive gain.



In summary, Bode stability analysis provides a method for determining the stability of most feedback control systems that include dead time. The calculations are relatively simple by hand when $G_{OL}(s)$ involves a series of individual transfer functions, and a computer can be programmed to perform the calculations automatically. In addition to providing a quantitative test, the Bode analysis yields insight into the effects on stability of various elements in the feedback loop.

10.7 □ CONTROLLER TUNING BASED ON STABILITY: ZIEGLER-NICHOLS CLOSED-LOOP

The Bode stability analysis provides a way to determine whether a process and feedback controller, with all elements completely specified, is stable. It is possible to alter the procedure slightly to determine, for a given process, the value of the gain for a *proportional-only* controller that results in a desired amplitude ratio for $G_{OL}(j\omega)$ at its critical frequency. In particular, it is straightforward to determine the controller gain that would result in the system being on the margin just between stable and unstable behavior. Note that the proportional-only controller affects the amplitude ratio but not the phase angle, thus making the calculation easier.

The importance of this approach is that the results of the calculation (the controller ultimate gain and critical frequency) can be used with tuning rules presented in this section to determine initial tuning for P, PI, and PID controllers. This tuning method is an alternative to the method presented in the previous chapter. While the tuning rules do not generally give as good performance as the Ciancone correlations for simple first-order-with-dead-time processes, the method in this section has two advantages:

1. It can be applied to processes that are not well modelled by first-order-with-dead-time models.
2. It provides considerable insight into the effects of all loop elements (process, instrumentation, and control algorithm) on stability and proper tuning constant values.

As with most tuning methods, the starting point is a process model that can be determined by fundamental modelling or by empirical model identification. The method then follows four steps.

1. Plot the amplitude ratio and the phase angle in the form of a Bode plot for $G_{OL}(s)$. At this step, the controller is a proportional-only algorithm with the gain K_c set to 1.0.
2. Determine the critical frequency ω_c and the amplitude ratio at the critical frequency, $|G_{OL}(j\omega_c)|$.
3. Calculate the value of the controller gain for a proportional-only controller that would result in the feedback system being at the stability margin. Since the stability margin is characterized by an amplitude ratio of 1.0 for $G_{OL}(j\omega_c)$, and K_c does not influence the critical frequency, the controller gain at the stability limit can be determined by first calculating the critical frequency and then calculating the controller gain.

$$\begin{aligned} \angle G_{OL}(j\omega_c) &= \angle G_p(j\omega_c)G_v(j\omega_c)G_s(j\omega_c) = -180^\circ \\ |G_{OL}(j\omega_c)| &= K_u |G_p(j\omega_c)G_v(j\omega_c)G_s(j\omega_c)| = 1.0 \end{aligned} \quad (10.39)$$

TABLE 10.4**Ziegler-Nichols closed-loop tuning correlations**

Controller	K_c	T_I	T_d
P-only	$K_u/2$	—	—
PI	$K_u/2.2$	$P_u/1.2$	—
PID	$K_u/1.7$	$P_u/2.0$	$P_u/8$

Ultimate gain:
$$K_u = \frac{1}{|G_p(j\omega_c)G_v(j\omega_c)G_s(j\omega_c)|} \quad (10.40)$$

Ultimate period:
$$P_u = \frac{2\pi}{\omega_c}$$

K_u , termed the *ultimate gain*, is the controller gain that brings the system to the margin of stability at the critical frequency. P_u , termed the *ultimate period*, is the period of oscillation of the system at the margin of stability. Note that K_u has the units of the inverse of the process gain $(K_p K_v K_s)^{-1}$ and that P_u has the units of time.

- Calculate the controller tuning constant values according to the Ziegler-Nichols closed-loop tuning correlations given in Table 10.4 (Ziegler and Nichols, 1942). The description “closed-loop” indicates that the analysis is based on the stability of the closed-loop feedback system, $G_{OL}(s)$. These correlations have been developed to provide acceptable control performance (they selected a 1:4 decay ratio) with reasonably aggressive feedback action; they believed that this also maintains the system a *safe margin from instability*.

EXAMPLE 10.10.

Calculate controller tuning constants for the three-tank mixing process in Example 7.2 by using the Ziegler-Nichols closed-loop method.

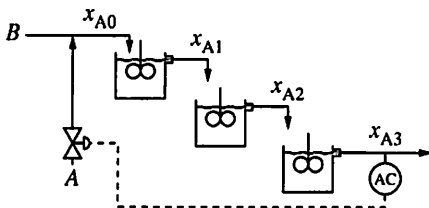
The transfer function for this process has already been developed, $G_p(s) = 0.039/(5s+1)^3$ and the Bode plot of the transfer function with ($K_c = 1$) is presented in Figure 10.14 based on

$$G_{OL}(s) = K_c \left(\frac{0.039}{(5s+1)^3} \right)$$

$$\angle G_{OL}(j\omega) = 3 \tan^{-1}(-5\omega)$$

$$|G_{OL}(j\omega)| = 0.039 \left(\frac{1}{\sqrt{1+5^2\omega^2}} \right)^3$$

If the plot were not available, the calculations would have to be performed by hand. They involve a trial-and-error procedure to determine the critical frequency and are often arranged in a table similar to the results in the following figure.



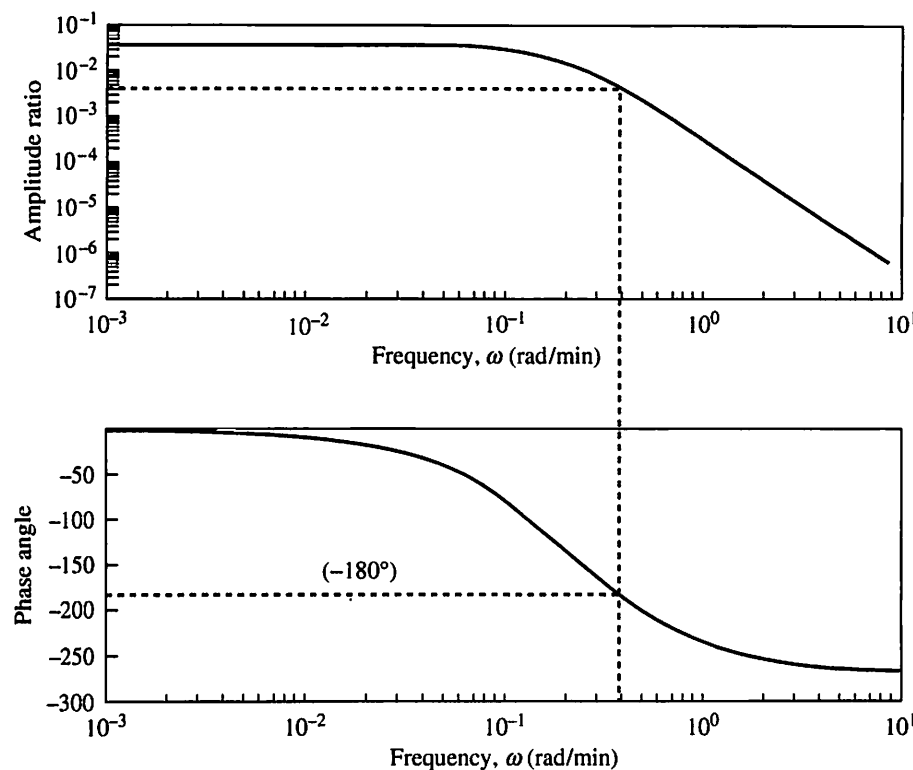
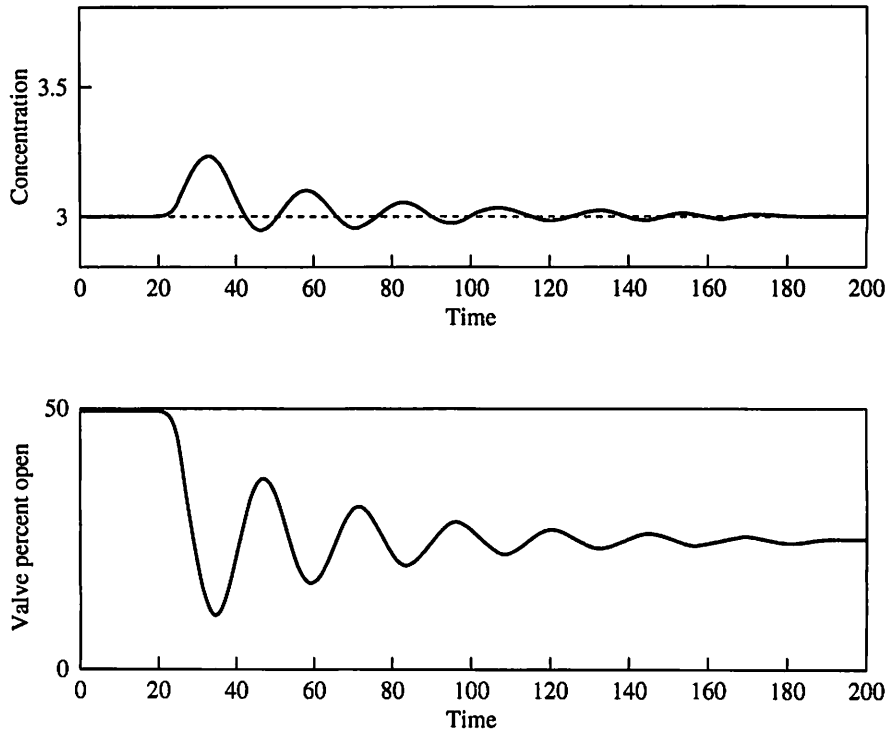


FIGURE 10.14
Bode plots of $G_{OL}(j\omega)$ for Example 10.10 with $K_c = 1$.

Frequency ω (rad/min)	Phase angle ϕ (°)	Amplitude ratio AR
0.10	-79.7	0.0279
0.20	-135	0.0138
0.35	-180.8 (critical frequency)	0.0048
0.40	-190.3	0.0035

From the results in the table, the ultimate gain and period can be determined to be $P_u = 2\pi/\omega_c = 17.9$ min and $K_u = 1/AR_c = 208$. The tuning constants for P, PI, and PID controllers according to the Ziegler-Nichols correlations are

Controller	K_c (% open/%A)	T_I (min)	T_d (min)
P-only	104	—	—
PI	94.5	14.9	—
PID	122.4	8.95	2.2

**FIGURE 10.15**

Dynamic response of three-tank mixing control system in Example 10.10 with Ziegler-Nichols tuning.

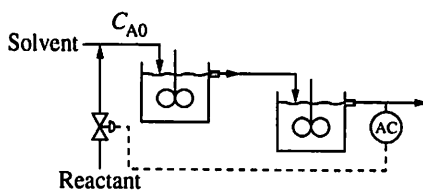
A sample of the transient response for a step change of +0.8%A in the feed concentration under PI control is given in Figure 10.15. As can be seen, the control performance is quite oscillatory, resulting in large variation in the manipulated variable and in a long settling time. For most plant situations, this is too oscillatory, and control performance for this system similar to Figure 9.6 would be preferred. The engineer could fine-tune the controller constants using the concepts presented in Section 9.6.

EXAMPLE 10.11.

Calculate tuning for a PI controller applied to the series chemical reactors in Example 10.8. Recall that this is a second-order-with-dead-time process with $G_p(s) = 0.10e^{-s}/(0.50s + 1)^2$.

The Bode plot for $G_{OL}(j\omega)$ with $K_c = 1$ is given in Figure 10.16. Note that the contribution of the individual elements in $G_{OL}(s)$ can be determined using the following relationships for transfer functions in series, equation (10.28):

$$\begin{aligned}\angle G_{OL}(j\omega) &= \angle \frac{1}{1 + 0.5j\omega} + \angle \frac{1}{1 + 0.5j\omega} + \angle e^{-1j\omega} + \angle (0.10) + \angle K_c|_{=1} \\ &= \tan^{-1}(-0.5\omega) + \tan^{-1}(-0.5\omega) - \omega \frac{360}{2\pi} + 0 + 0\end{aligned}$$



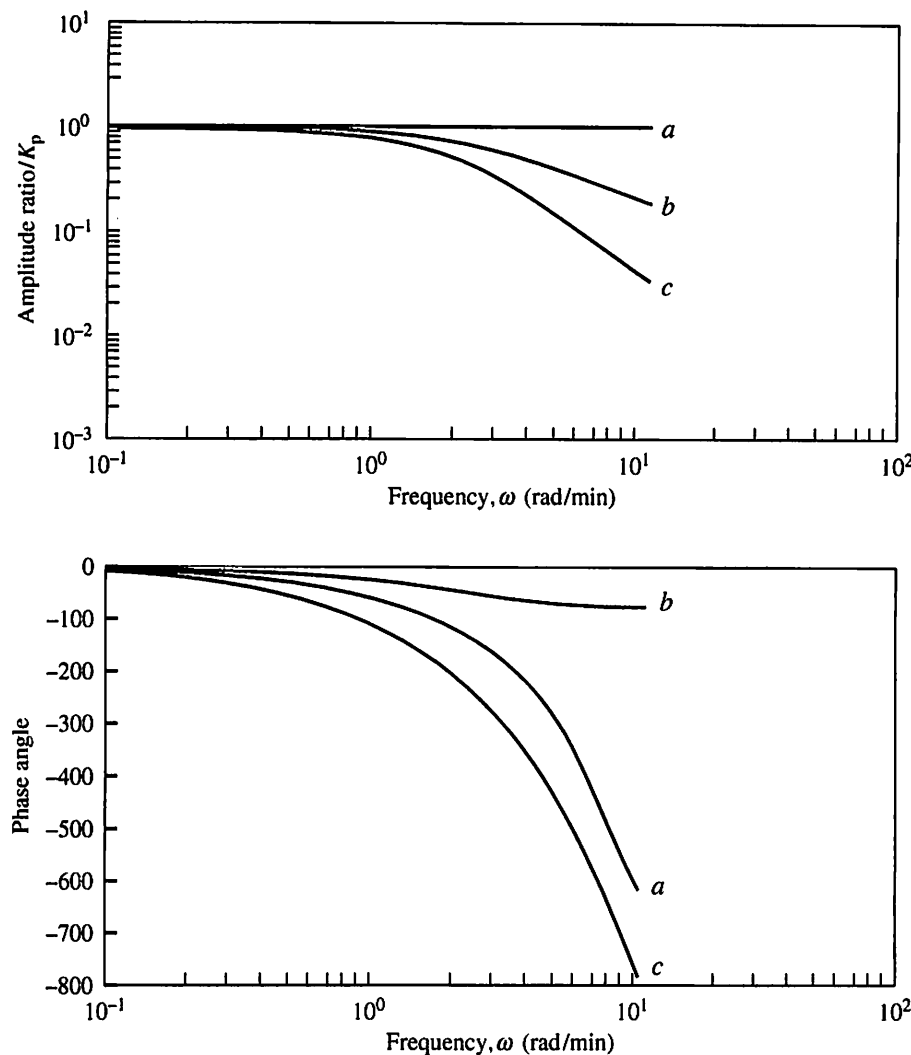


FIGURE 10.16

Bode plot of Example 10.11 with $K_c = 1$; for (a) the dead time, (b) one first-order system, and (c) the entire transfer function $G_{OL}(j\omega)/K_p$.

$$\begin{aligned}|G_{OL}(j\omega)| &= \left| \frac{1}{1 + 0.5j\omega} \right| \left| \frac{1}{1 + 0.5j\omega} \right| |e^{-j\omega}| |0.10| |K_c|_{=1}| \\ &= \sqrt{\frac{1}{1 + 0.25\omega^2}} \sqrt{\frac{1}{1 + 0.25\omega^2}} (1.0)(0.10)(1.0)\end{aligned}$$

The results in Figure 10.16 are presented so that the effects of the individual process elements are clearly displayed. The dead time and one first-order system are designated as *a* and *b*, respectively. The overall amplitude ratio and phase angle for $G_{OL}(j\omega)$ can be determined from the foregoing equations. When the frequency responses of the individual elements are presented in the Bode plot, the overall amplitude ratio is the *sum* of the distances on the plot of the individual deviations from 1.0, since the amplitude ratio is plotted on a log scale. Also, the total phase angle is the *sum* of the distances on the plot of the individual deviations from zero degrees, since the phase angle is plotted on a linear scale. These rules

are not particularly important as far as simplifying the calculations, which are easily programmed; however, they help the engineer visualize the effects on stability of individual elements in the feedback loop. For example, any element that contributes a large phase lag itself will cause a large phase lag for $G_{OL}(j\omega)$. From this figure, the critical frequency is 1.73 rad/min and the magnitude at this frequency is 0.057; thus, the controller tuning would be, according to the Ziegler-Nichols tuning correlations in Table 10.4, $K_c = 8.0\%$ open/(mole/m³) and $T_i = 3.0$ min.

Before this section is concluded, two common questions are addressed. First, the novice often has difficulty in selecting an initial frequency for the trial-and-error calculation for the critical frequency. Since an exact guess is not required, a good initial estimate can usually be determined from the relationships in Tables 10.2 and 10.3, along with the plots in Figure 10.13. Basically, the initial frequency should be taken in the region where the Bode diagrams of the individual elements change greatly with frequency. Rough initial estimates for the frequency are given by the following expressions:

$$\begin{aligned}\omega\tau &= 1 && \text{(first-order system)} \\ \omega\tau &= 1 && \text{(second-order system)} \\ \omega\theta &= 1 && \text{(dead time)}\end{aligned}$$

When these calculations give very different results, use the lowest of the estimated frequencies to begin the trial-and-error calculations, which usually converge quickly.

The second common question regards the required accuracy of the converged answer. The engineer must always consider the accuracy of the information used in a calculation when interpreting the results. In Chapter 6, the results of empirical model fitting were found to have significant errors, usually 10 to 20 percent in all parameters. Therefore, it is not necessary to determine the critical frequency so that the phase angle deviation from -180° is less than 0.001° ! A few degrees error is usually acceptable. In addition, our application of the results in determining tuning constants must consider the likely error in the model, as discussed in the next section.

10.8 □ CONTROLLER TUNING AND STABILITY—SOME IMPORTANT INTERPRETATIONS

Analysis using the Bode plots provides a quantitative method for evaluating how elements in the control loop influence stability and tuning. The principles and examples presented so far have demonstrated important results, which are reinforced in the following six interpretations, discussed with further examples. The reader is advised that these interpretations are very important, not only in tuning single-loop controllers but also in designing more complex control strategies and process modifications to achieve desired control performance.

Interpretation I: Effect of Process Dynamics on Tuning

Clearly, the types of process and instrument equipment in the control loop affect the system stability and feedback tuning constants. It is worthwhile determining

how process dynamics affect feedback control, specifically the gain and integral time of a PI controller. Since the ultimate gain of the proportional-only controller is the inverse of the amplitude ratio at the critical frequency, a higher controller gain for a stable system is achieved by decreasing the amplitude ratio at the critical frequency. Also, the amplitude ratio generally decreases for process elements as the frequency increases. Therefore, smaller time constants and dead times lead to a larger allowable controller gain. By the same logic, smaller values of the time constants and dead times lead to a smaller integral time, which, since integral time appears in the denominator, has the effect of giving stronger control action. The general conclusion is that more and longer time constants and dead times lead to detuning of the PID controller and that fewer and shorter time constants and dead times lead to larger controller gain, smaller integral time, and stronger feedback action. We expect that stronger feedback action will give better control performance, as is discussed in depth in Chapter 13.

EXAMPLE 10.12.

Consider a set of processes with one to seven first-order systems in series, each with a gain of 1.0 and a time constant of 5.0. Determine the PI tuning for each of these systems.

The expressions for the amplitude ratio and phase angle for a series of n first-order systems can be developed using equations (5.40) and (10.36) and are given as

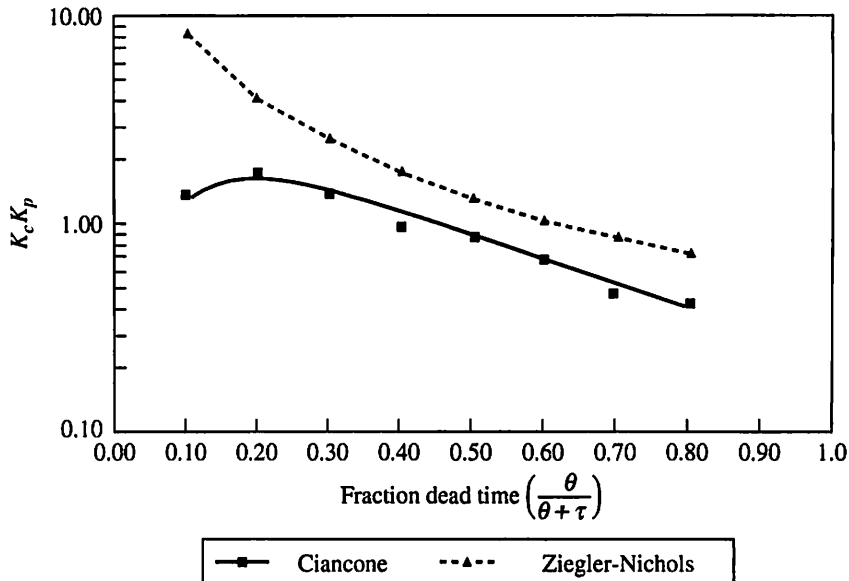
$$AR = \left(\frac{K_p}{\sqrt{1 + \omega^2 \tau^2}} \right)^n \quad \phi = n \tan^{-1}(-\omega\tau) \quad \text{with } K_p = 1.0 \quad \text{and} \quad \tau = 5.0$$

The Ziegler-Nichols closed-loop tuning for these systems is as follows:

n	ω_c	$AR _{\omega_c}$	K_c	T_I
1	∞	—	∞	—
3	0.35	0.122	3.72	15.0
5	0.145	0.348	1.31	36.1
7	0.096	0.484	0.94	54.5

Clearly, the controller must be detuned as the feedback dynamics become slower.

The previous example clearly demonstrates that time constants affect feedback tuning and stability. Next, we would like to learn the relative importance of dead times and time constants. Since many processes can be represented by a first-order-with-dead-time model, the key relationships between tuning and fraction dead time $\theta/(\theta + \tau)$ is investigated for Ziegler-Nichols PID tuning. In fact, correlations similar to those developed in Chapter 9 can be calculated using the Bode stability and Ziegler-Nichols methods. The PID controller gain correlations for Ciancone and Ziegler-Nichols are compared in Figure 10.17. The correlations have the same general shape, which points to the importance of the stability limit

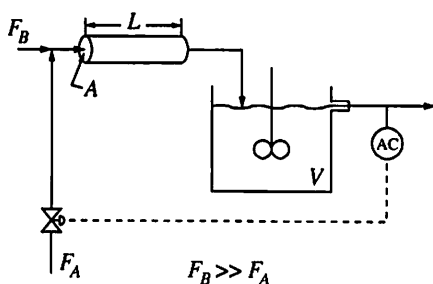
**FIGURE 10.17**

The effect of fraction dead time on PID controller gain with $\theta + \tau$ constant.

in determining the most aggressive control action. Recall that stability was not explicitly considered in the Ciancone method, although tuning that gave unstable or oscillatory systems would have a large IAE and thus would not have been selected as optimum. Note that the Ciancone gain values are lower, partly because of the objectives of robust performance with model errors and partly because of the limitation on manipulated-variable variation with a noisy measured controlled variable. We would expect the Ciancone correlations to yield controllers that are more robust than those developed with Ziegler-Nichols tuning and thus perform better when realistic model errors occur.

The Bode analysis demonstrates the fundamental relationship between fraction dead time and tuning; the controller gain must be decreased to maintain stability as the fraction dead time increases (at constant $\theta + \tau$). Finally, it is important to reiterate that only the terms in the characteristic equation influence stability. Therefore, the disturbance transfer function $G_d(s)$ and the manner in which the set point is changed do not influence the stability of the feedback control system.

Increasing time constants and dead times requires detuning of the PID controller. The dead time has a greater effect on the phase lag and tuning. Therefore, increasing the fraction dead time, $\theta / (\theta + \tau)$, at constant $\theta + \tau$ requires detuning of the PID controller.

**EXAMPLE 10.13.**

The two following different first-order-with-dead-time processes are to be controlled by PI controllers. Calculate the tuning constants for each and compare the results.

Controller Tuning and
Stability—Some
Important
Interpretations

	Plant A	Plant B
K_p	1.0	1.0
τ	8.0	2.0
θ	2.0	8.0

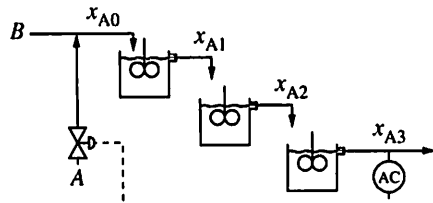
For each plant the Bode stability and Ziegler-Nichols tuning calculations are summarized as

	Plant A	Plant B
ω_c	0.86	0.32
AR_c	0.144	0.84 (P-only with $K_c = 1$)
K_u	6.94	1.19
P_u	7.3	19.60
K_c	4.1	0.70
T_I	3.65	9.8
T_d	0.91	2.45

Note that the two plants have the same time to reach 63% of their open-loop response after a step change: $\theta + \tau$. Even though they have the same "speed" of response, Plant B, with the higher fraction dead time, $\theta/(\theta + \tau)$, has a much smaller controller gain and larger integral time. The difference in controller tuning constants, resulting from the different stability bound, certainly will result in poorer control performance for Plant B. (Naturally, the longer dead time for plant B also degrades the control performance.)

Interpretation II: Effect of Controller Modes on Stability

Each mode of the PID controller affects the stability of the feedback system. As shown in Figure 10.13a, a gain in $G_{OL}(s)$ does not affect the phase angle, although it affects the amplitude ratio. Therefore, increasing the magnitude of the controller gain tends to *destabilize* the system; that is, move it toward an amplitude ratio greater than 1. The proportional-integral controller shown in Figure 10.13f affects both the amplitude ratio and the phase angle; it increases the amplitude ratio beyond the proportional-only controller and increases the phase lag. Thus, increasing the gain and decreasing the integral time tend to *destabilize* the feedback system. The proportional-derivative controller shown in Figure 10.13g increases the amplitude ratio but contributes negative phase lag, referred to as *phase lead*. Therefore, the derivative mode tends to *stabilize* the feedback system. These qualitative results are reflected in the Ziegler-Nichols tuning rules, which show the controller gain decreasing from P-only to PI control and increasing from PI to PID control.



EXAMPLE 10.14.

The stability of the three-tank mixing process is to be determined for two cases: (a) under proportional-only feedback control ($K_c = 122$) and (b) under proportional-integral feedback control ($K_c = 122$ and $T_I = 8$). Note that the controller gain is the Ziegler-Nichols value for the PID controller from Example 10.10, but the integral time is slightly different and the derivative time is 0.

The Bode plots are presented in Figure 10.18a and b. From Figure 10.18a, it is determined that case (a) is stable, since the amplitude ratio (0.60) is less than 1.0 at the critical frequency (0.35 rad/min). From Figure 10.18b, it is determined that case (b) is unstable, because it has an amplitude ratio greater than 1.0 (1.3) at its critical frequency (0.25 rad/min). This result clearly demonstrates the effect of the integral mode, which tends to destabilize the control system, since it contributes phase lag. Remember that the integral mode is nearly always retained, in spite of its tendency to destabilize the control system, because it ensures zero steady-state offset.

Interpretation III: Effect of Modelling Errors on Stability

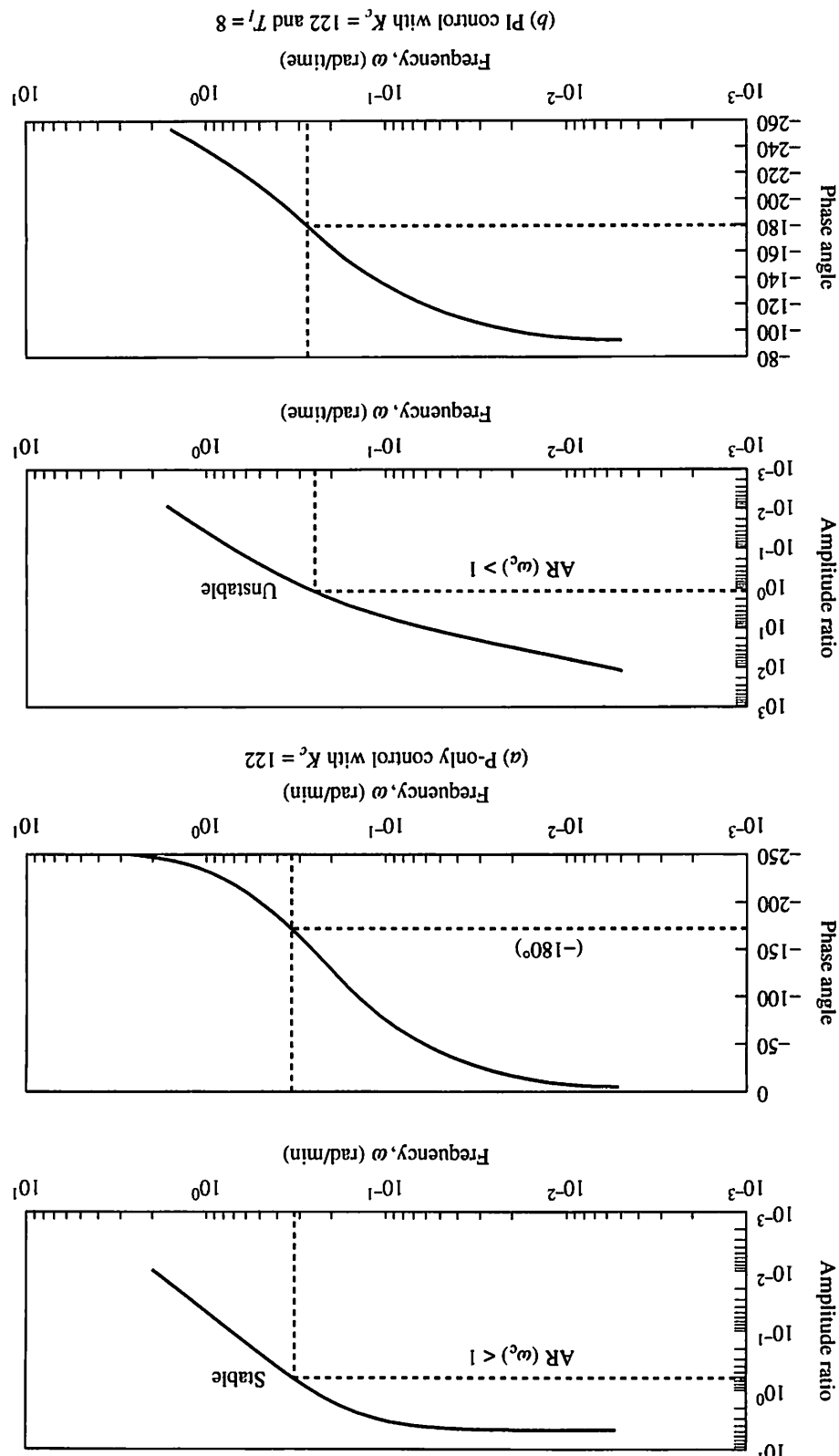
The preceding examples in this chapter have assumed that the models of the process were known exactly. Since the true dynamic response is never known exactly, it is important to determine how model errors affect stability. The best estimate of the dynamics will be called the *nominal model*. The general trends are relatively easy to ascertain based on the Bode stability analysis; plants with amplitude ratios and phase lags greater than their nominal models will be closer to the stability margin than the nominal model. As an example, consider a first-order-with-dead-time process. Assuming that a nominal model is used to calculate the tuning constants, the system will tend to be closer to the stability margin than predicted if (1) the actual process dead time is greater than the nominal model, (2) the process gain is greater than the nominal model, or (3) the process time constant is greater than the nominal model.

A consideration of modelling errors should be an integral part of any controller tuning method. The time-domain Ciancone method in Chapter 9 specified modelling errors and optimized the dynamic responses for several cases simultaneously, and the Ziegler-Nichols correlations included a factor for model error by reducing the amplitude ratio at the critical frequency to about 0.5. As a result, a combination of model errors would have to cause the actual amplitude ratio at the critical frequency to be about twice the nominal model value for the system to be unstable. An alternative to the Ziegler-Nichols guideline for tuning based on the stability limit explicitly considers a measure of potential error. This method adjusts the controller tuning constant values so that the system is on the stable side of the limit by a specified amount. Either of the following specifications is used.

GAIN MARGIN. The amplitude ratio of $G_{OL}(j\omega)$ at the critical frequency is equal to $1/GM$, where GM is called the *gain margin* and should be greater than 1. This ensures that the system is stable for any process modelling error that increases

Bode plots of $G_{\text{OL}}(j\omega)$ for Example 10.14.

FIGURE 10.18



the actual amplitude ratio of the process by less than a factor of GM. A typical value for GM is 2.0, but a larger value would be appropriate if large modelling errors that primarily influenced the amplitude ratio were anticipated.

PHASE MARGIN. The phase angle of $G_{OL}(j\omega)$ where the amplitude ratio is 1.0 is equal to $(-180^\circ + PM)$, with PM a positive number referred to as the *phase margin*. A positive phase margin ensures that the system is stable for model errors that decrease the phase angle. A typical value for the phase margin is 30° , but a larger value would be appropriate if larger modelling errors were anticipated.

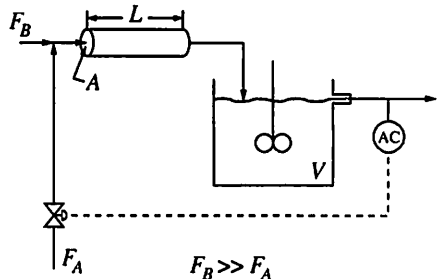
Even if the models were perfect, the values of the gain margin and phase margin should not be reduced much below 2.0 and 30° , respectively. If they were reduced further, the performance of the feedback control system would be poor (i.e., highly oscillatory), because the roots of the characteristic equation would be too near the imaginary axis. Thus, these margins can be used as a way to include additional conservatism in the Ziegler-Nichols tuning methods if large model errors are expected.

EXAMPLE 10.15.

A nominal model for a process is given along with parameters defining processes I and II, which represent the range of the true process dynamics experienced as operating conditions vary. Naturally, we never know the true process, but we can usually estimate the potential deviations between the nominal model and true process from an analysis of repeated model identification experiments and from fundamental models, which indicate how the process dynamics change with, for example, the flow rate.

(a) Determine values for the PI tuning constants based on the Ziegler-Nichols method for the nominal model and determine the resulting gain and phase margins.

(b) Determine the stability of the true process at the extremes of its parameter ranges using the tuning based on the nominal model.



Nominal model	True process	
	I	II
K_p	1.0	1.0
τ	9.0	9.5
θ	1.0	0.5

Tuning can be determined for the nominal model using the Bode and Ziegler-Nichols closed-loop methods, giving the following results:

$$G_{OL}(s) = K_c \left(\frac{1.0e^{-s}}{9s + 1} \right) \quad \text{with } K_c = 1.0$$

$$\omega_c = 1.65 \quad |G_{OL}(j\omega_c)| = 0.067 \quad K_u = 14.9$$

$$K_c = 6.8 \quad T_I = 3.2 \quad \text{Gain margin} = 2.0 \quad \text{Phase margin} = 30^\circ$$

The tuning constants appropriate for the nominal model using the Ziegler-Nichols method, that satisfy the general guidelines for gain and phase margins, are now

applied to the extremes of the dynamics of the true process.

$$G_{OL}(s) = 6.8 \left(1 + \frac{1}{3.2s}\right) \frac{1.0e^{-0s}}{\tau s + 1}$$

True process with PI control

	I	II
ω_c	3.1	0.66
AR_c	$0.23 < 1$	$1.39 > 1$

Note that Process I is stable with the nominal tuning, whereas Process II is unstable. The general trend should be expected, since Process II has a longer dead time, which contributes substantial phase lag and is more difficult to control. Process I has a shorter dead time, which contributes less phase lag and is easier to control. The key point is that the control system would become unstable for the moderate amount of variation of Process II from the nominal model.

Thus:

The control engineer should not rely exclusively on general tuning guidelines but should include information on the expected variation in process dynamics when tuning controllers.

The goal is normally for the *worst-case* model error to be stable and to give an acceptable (usually stable and not too oscillatory) closed-loop dynamic response. Further calculations for Example 10.15 indicate that gain and phase margins for the *nominal model* of 4 and 60° , respectively, were required to give satisfactory performance for Process II. (This tuning gave gain and phase margins of 2 and 40° , respectively, for Process II.)

The need for a larger stability margin can be understood when the Bode plot is prepared using the entire range of models possible, not just the nominal model. The range of possible models depends on the reasons for model errors; here the simplest approach is taken, with the process models I and II defining the extremes of the amplitude and phase angles possible. The Bode plot of $G_{OL}(s) = G_c(s)G_p(s)$, with the PI controller tuning for the nominal plant from Example 10.15, gives the range of values in Figure 10.19. Any amplitude ratio and phase angle within the two lines are possible for the assumed uncertainty. This plot clearly shows the effects of model errors, the possibility for instability in this case, and the need for a (larger) safety margin to account for the error. (Other ways to characterize the model error link the variation in process operation to the change in dynamics; for example, see Chapter 16.)

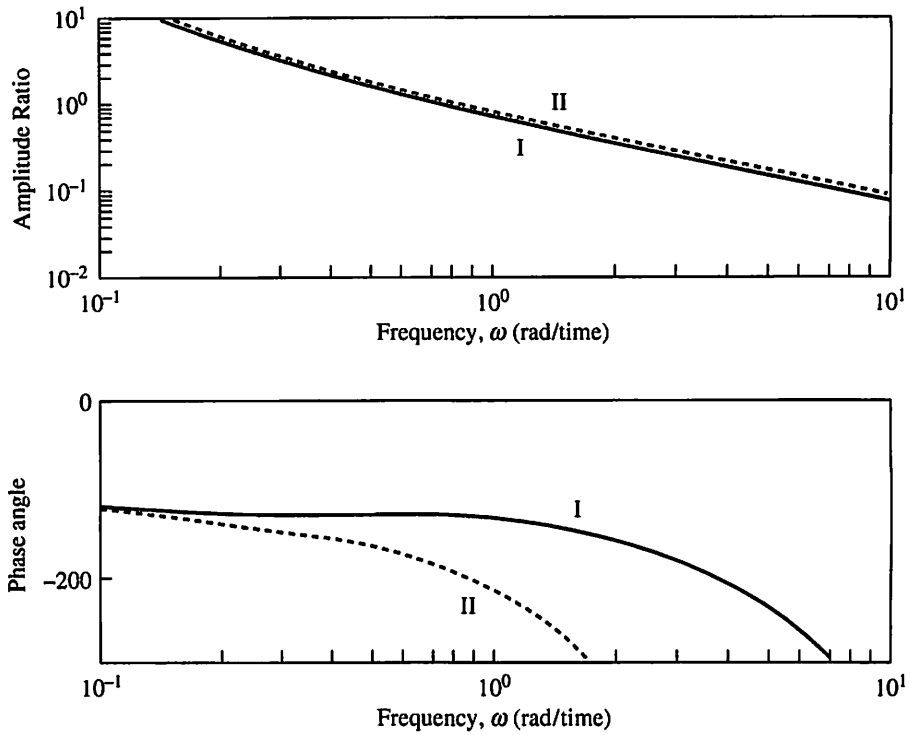


FIGURE 10.19

Uncertainty in Example 10.15 defined by models I and II with tuning for the nominal model.

Interpretation IV: Experimental Tuning Approach

The Bode tuning method enables the engineer to calculate the proportional controller gain that brings the system to the stability limit. The same principle could be used to determine the ultimate gain experimentally through a simple trial-and-error procedure called *continuous cycling*. The real physical system would be controlled by a proportional-only controller, the set point perturbed slightly, and the transient response of the controlled variable observed. If the system is stable, either over-damped or oscillatory, the gain is increased; if unstable, the gain is decreased. The iterative procedure is continued, changing K_c until after a set point perturbation, the system oscillates with a constant amplitude. This behavior occurs when the system has exponential terms with (very nearly) zero values for their real parts, indicating that the system is at the stability margin. The gain at this condition is the ultimate gain, and the frequency of the oscillation is the critical frequency. These values, which in the continuous cycling procedure have been determined empirically, can be used with the Ziegler-Nichols closed-loop tuning correlations in Table 10.4 for calculating the PID constants. From this explanation, it should be clear why the correlations used in this section are called the “closed-loop” continuous cycling correlations. Also, we should recognize that this method combines an experimental identification method with tuning recommendations. This experimental method is *not recommended*, because of the significant, prolonged disturbances introduced to the process. It is presented here to give a physical, time-domain meaning to the Bode stability calculations.

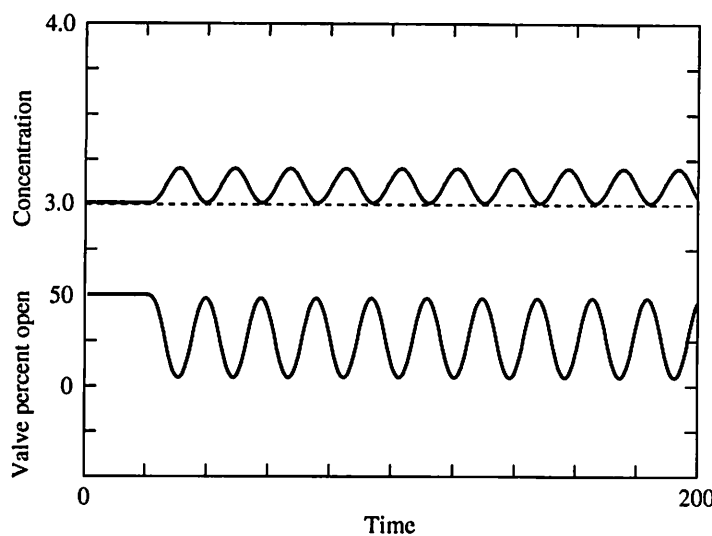


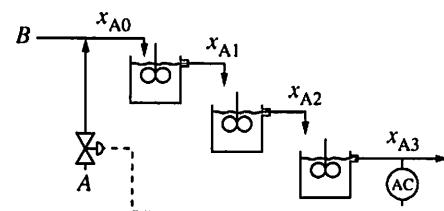
FIGURE 10.20

Dynamic response of three-tank mixing process with proportional-only controller and $K_c = 206$, the ultimate gain.

EXAMPLE 10.16.

Perform the empirical continuous cycling tuning method on the three-tank mixing process.

The resulting dynamic response at the stability limit is given in Figure 10.20. The controller gain was found by trial and error to be 206 and the period to be about 18 minutes. These are essentially the same answers as found in Example 10.10, where the three-tank mixing process was analyzed using the Bode method.



Interpretation V: Relationship between Stability and Performance

The analysis of roots of the characteristic equation $1 + G_{OL}(s) = 0$ and, equivalently, Bode plots of $G_{OL}(s)$ provide methods for determining the stability of linear systems. Naturally, any feedback control system must be stable if it is to provide good control performance. However, stability is not sufficient to guarantee good performance. To see why, consider the closed-loop transfer function for a disturbance response:

$$\frac{CV(s)}{D(s)} = \frac{G_d(s)}{1 + G_c(s)G_p(s)} \quad \text{or} \quad CV(s) = \frac{G_d(s)}{1 + G_c(s)G_p(s)} D(s) \quad (10.41)$$

The stability analysis considers the *denominator* in the characteristic equation, $1 + G_c(s)G_p(s)$. Naturally, control performance also depends on the disturbance size and dynamics that appear in the numerator of the transfer function. For example, the three-tank mixing process would certainly remain closer to the set point

for an inlet concentration disturbance of 0.01% in stream *B* compared to a 1% disturbance. Also, the system is stable when the feedback controller gain has a value of 0.1, which would give very poor control performance compared with the tuning determined in Example 10.10 for this process ($K_c = 94.5$). Clearly, the methods in this chapter, while providing essential stability information, do not provide all the information required for process control design. Control system performance is covered in more detail in Chapter 13.

Stability is required for good control system performance. However, a control system can be stable and perform poorly.

EXAMPLE 10.17.

Determine how the control performance changes for the following process with different disturbance dynamics.

$$G_p(s) = \frac{0.039}{(1+5s)^3} \quad G_d(s) = \frac{1}{(1+\tau_d s)^n} \quad (10.42)$$

with $\tau_d = 5$ and n equal to (a) 3 and (b) 1.

The system was simulated with a PI controller using the tuning from Example 10.10. The two different disturbance transfer functions given here were considered. The first case (a) is the standard three-tank mixing system, and the dynamic response is given in Figure 10.15. The results for the faster disturbance, case (b), are given in Figure 10.21. As expected, the faster the disturbance enters the process, the poorer the feedback control system performs. Remember, the two cases considered in this example have the same relative stability because the feedback dynamics $G_p(s)$ and the controller G_c are identical; only the disturbances are different. (Also, note that the valve goes below 0% open in the simulation of the

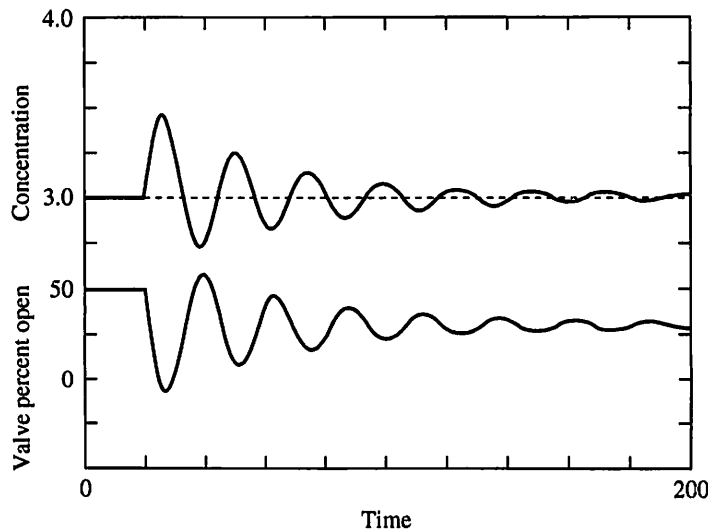


FIGURE 10.21

Dynamic response for the system in Example 10.17, case (b) (faster disturbance).

linearized model, which is not physically possible; a nonlinear simulation should be performed.)

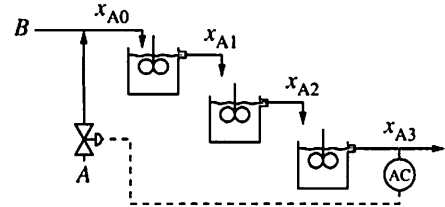
Interpretation VI: Modelling Requirement for Stability Analysis

We use approximate models for control system analysis and design, and we should select the model that provides an adequate representation of the dynamic behavior required by the analysis method. The Bode stability analysis has pointed out the extreme importance of model accuracy *near the critical frequency*. Thus, we do not require a model that represents the process accurately at high frequencies—that is, those frequencies much higher than the critical frequency.

EXAMPLE 10.18.

Compare the frequency responses for the three-tank mixing process derived from (a) fundamentals and (b) empirical model fitting.

The linearized fundamental model derived in Example 7.2 and repeated in equation (10.42) is third-order, and the empirical model is a first-order-with-dead-time (approximate) model in Example 6.4. Their frequency responses, which equal $G_{OL}(s)$ with $G_c(s) = K_c = 1$, are given in Figure 10.22. Note that the two frequency responses are quite close at low frequencies, since they have the same steady-state gains. At very high frequencies, they differ greatly, but we are not interested in that frequency range. Near the critical frequency ($\omega_c \approx 0.35$), the models do not differ greatly, which indicates that the two models give similar, but not exactly the same, tuning constants. Since essentially no model is perfect, we conclude that the error introduced by using a first-order-with-dead-time model approximation is often acceptably small for the purposes of calculating initial tuning constant values. Recall that further tuning improvements are made through fine tuning.



In summary, tuning methods were presented in this section that are based on margins from the stability limit. The method can be applied to any stable process with a monotonic relationship between the phase angle and frequency. The methods in this section are especially helpful in determining the effects of various process and controller elements on the tuning constants.

10.9 □ ADDITIONAL TUNING METHODS IN COMMON USE, WITH A RECOMMENDATION

To this point, two controller tuning methods have been presented. The Ciancone correlations were based on a comprehensive definition of control performance in the time domain, whereas the Ziegler-Nichols closed-loop method was based on stability margin. Many other tuning methods have been developed and reported in the literature and textbooks. A few of the better known are summarized in this section, along with a recommendation on the methods to use.

One well-known method, known as the Ziegler-Nichols *open-loop* method (Ziegler and Nichols, 1942), provides correlations that can be used with simplified process models developed from such sources as an open-loop process reaction

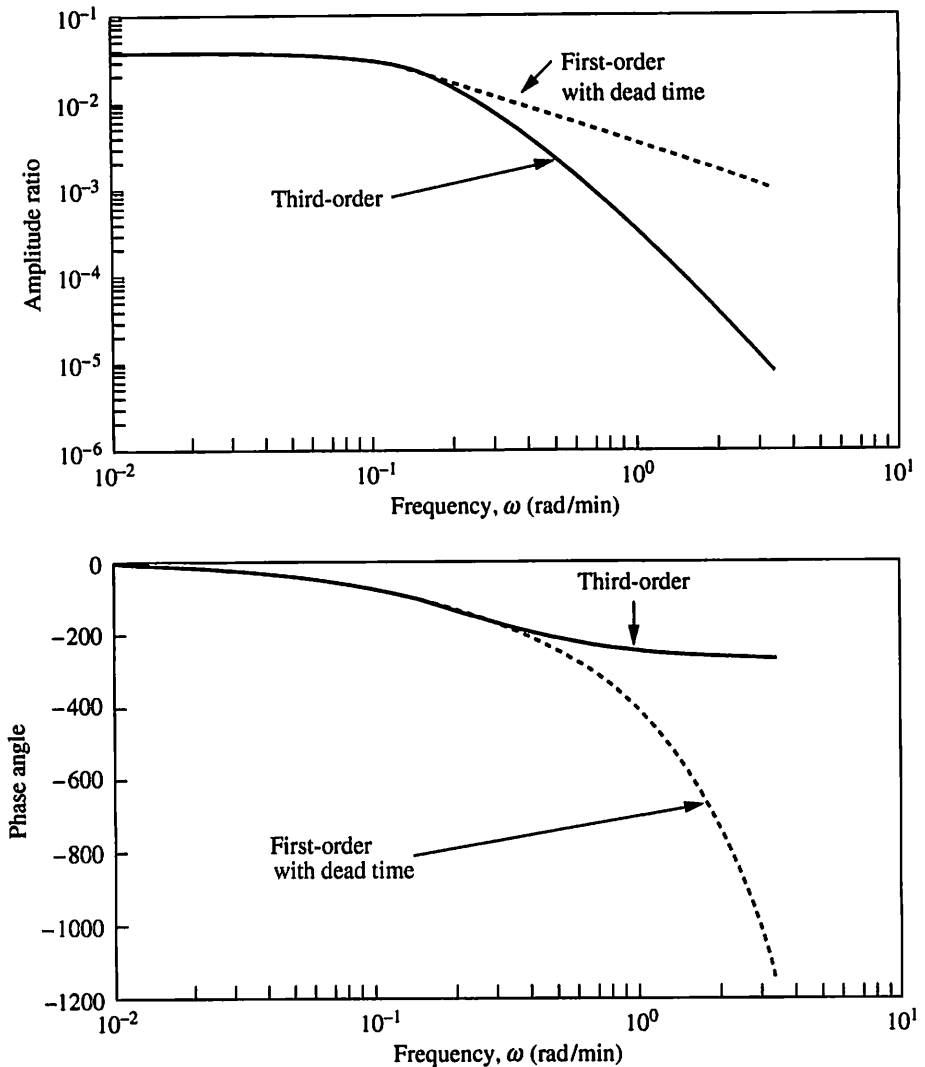


FIGURE 10.22

Comparison of Bode plots for exact and approximate process models.

curve. The objective of these correlations is a 1:4 decay ratio for the controlled variable. The tuning constants are calculated from the experimental model parameters according to the expressions in Table 10.5. Notice that the dead time is in the denominator of the calculation for the controller gain. This indicates that the controller gain should decrease as the dead time increases, a result consistent with other tuning methods already considered. However, the open-loop Ziegler-Nichols correlation predicts a very large controller gain for processes with small dead times and an infinite gain for processes with no dead time. These results will lead to excessive variation in the manipulated variable and to a controller with too small a stability margin. Therefore, these correlations should not be used for processes with small fraction dead times.

Many other tuning methods have been developed, generally based on either stability margins or time-domain performance. A summary of the methods is presented in Table 10.6, which gives the main objectives of each method, along with a reference, either in this book or in the literature. Note that the IMC method is covered in Chapter 19.

TABLE 10.5**Ziegler-Nichols open-loop tuning based on process reaction curve**

	K_c	T_I	T_d
P-only	$(1/K_p)(\tau/\theta)$	—	—
PI	$(0.9/K_p)(\tau/\theta)$	3.3θ	—
PID	$(1.2/K_p)(\tau/\theta)$	2.0θ	0.5θ

Additional Tuning Methods in Common Use, With a Recommendation

TABLE 10.6**Summary of PID tuning methods**

Tuning method	Stability objective	Objective for $CV(t)$	Objective for $MV(t)$	Model error	Noise on $CV(t)$	Input SP = set point D = disturbance
Ciancone (Chapter 9)	None explicit	Min IAE	Overshoot and variation with noise	±25%	Yes	SP and D individually
Fertik (1974)	None explicit	Min ITAE with limit on overshoot	None	None explicit	No	SP and D individually
Gain/phase margin (Section 10.8)	Gain margin or phase margin	None	None	Depends on margins	No	n/a
IMC tuning (Section 19.7)	For specified model error	ISE (robust performance)	None	Tune λ , see Morari and Zafiriou (1989)	No	SP and D (step and ramp) individually
Lopez et al. (1969)	None explicit	IAE, ISE, or ITAE	None	None	No	SP and D individually
Ziegler-Nichols closed-loop (Section 10.7)	Implicit margin for stability ratio ($GM \approx 2$)	4 : 1 decay ratio	None	None explicit	No	n/a
Ziegler-Nichols open-loop (Section 10.9)	Implicit margin for stability ratio ($GM \approx 2$)	4 : 1 decay ratio	None	None explicit	No	n/a

With such a large selection available, some recommendations are needed to assist in the proper choice of tuning method. Before presenting recommendations, a few key factors should be reiterated. First, most tuning methods rely on a simplified dynamic model of the open-loop process. As a result, good control performance from the tuning depends on reasonably accurate model identification. Tuning calculations cannot correct for modelling errors; they can only reduce the detrimental effects of such errors. Second, the tuning constants should be determined so

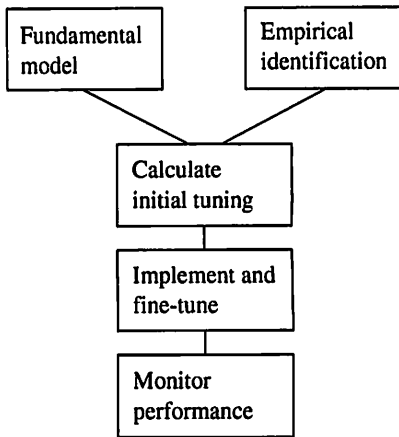


FIGURE 10.23

Major steps in the tuning procedure.

that the control system achieves desired performance objectives relevant to the process. Because each method has different objectives, each provides somewhat different dynamic performance, which should be matched to the process requirements. Third, all methods provide initial values, which should be fine-tuned based on plant experience; the tuning procedure shown in Figure 10.23 should be used. The tuning methods being discussed appear as the “initial tuning” that relies on the identification and is modified by fine tuning, which corrects for modelling errors and adapts the performance to that desired for the process.

The proper selection for a particular application should follow from the information in the table. In other words:

The best choice for the initial tuning correlation is the method that was developed for objectives conforming most closely to those of the actual situation for which the controller is being tuned.

The following ranking, with the first entry being the preferred method, represents the author’s personal preference for calculating initial tuning.

1. Ciancone tuning correlations from Chapter 9
2. Bode/(closed-loop) Ziegler-Nichols when process cannot be satisfactorily fitted by a first-order-with-dead-time model
3. Nyquist/gain margin when the process does not satisfy the Bode criteria
4. Any of the other correlations as appropriate for the application scenario
5. Detailed analysis of the robustness of the system, through either the optimization method in Chapter 9 or the robust performance analysis described in Morari and Zafiriou (1989)

Approach 5 would always be the best, but it requires more effort than is usually justified for initial tuning. However, it may be required for systems involving complex dynamics and large model errors.

10.10 CONCLUSIONS

Several important topics have been covered in this chapter that are essential for a complete understanding of dynamic systems. We have learned

1. A useful definition of stability related to poles of the transfer function, i.e., the exponents in the solution of a set of linear differential equations
2. The effects of process and control elements in the feedback path that affect stability, such as dead times and time constants
3. Tuning methods based on a margin from the stability limit
4. That model errors must always be considered in tuning and that this results in detuned (i.e., less aggressive) feedback control action

All of these results are consistent with the experience gathered in Chapter 9, which was restricted to first-order-with-dead-time processes and PID control. The methods in this chapter provide a valuable theoretical basis that helps us understand

time-domain behavior and that can be applied for quantitatively analyzing stability and determining tuning for a wide range of systems. Numerical examples in this chapter, as well as Chapter 9, have demonstrated that simple linear models are often adequate for calculating initial tuning constants. These results confirm that the first-order-with-dead-time models from empirical model fitting provide satisfactory accuracy for this control analysis.

The stability analysis methods presented in this chapter are summarized in Figure 10.24, which gives a simple flowchart for the selection of the appropriate method for a particular problem. Note that the direct analysis of the roots of the characteristic equation is applicable to either open- or closed-loop systems that have polynomial characteristic equations. The Bode method can be applied to most closed-loop systems, and the Nyquist method is the most general.

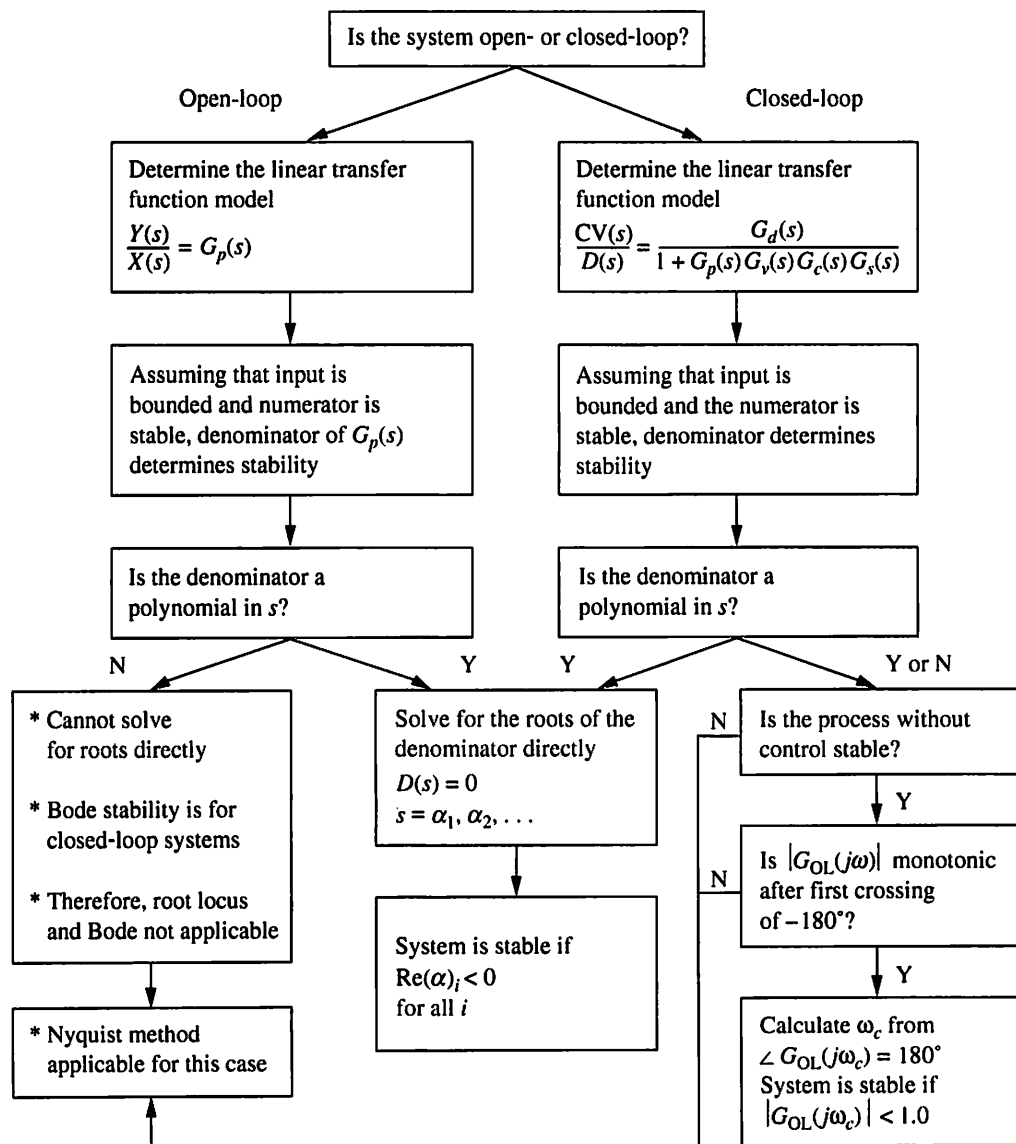


FIGURE 10.24

Flowchart for selecting the stability analysis method for local analysis using linearized models.

Many controller tuning methods have been presented in these two chapters. The correct method for a particular application depends on the objectives of the control system. The information in Table 10.6 will enable you to match the tuning with the control objectives. If no specific information is available, the Ciancone tuning correlations in Chapter 9 are recommended for initial tuning constant values.

REFERENCES

- Boyce, W., and R. Diprima, *Elementary Differential Equations*, Wiley, New York, 1986.
- Dorf, R., *Feedback Control Systems Analysis and Synthesis*, McGraw-Hill, New York, 1986.
- Fertik, H., "Tuning Controllers for Noisy Processers," *ISA Trans.*, 14, 4, 292–304 (1974).
- Franklin, G., J. Powell, and A. Emami-Naeini, *Feedback Control of Dynamic Systems* (2nd ed.), Addison-Wesley, Reading, MA, 1991.
- Lopez, A., P. Murrill, and C. Smith, "Tuning PI and PID Digital Controllers," *Intr. and Contr. Systems*, 89–95 (February 1969).
- MathWorks, The Mathworks, Inc., Cochituate Place, 24 Prime Park Way, South Natick, MA, 1998.
- Morari, M., and E. Zafiriou, *Robust Process Control*, Prentice-Hall, Englewood Cliffs, NJ, 1989.
- Perlmutter, D., *Stability of Chemical Reactors*, Prentice-Hall, Englewood Cliffs, NJ, 1972.
- Willems, J., *Stability Theory of Dynamical Systems*, Thomas Nelson and Sons, London, 1970.
- Ziegler, J., and N. Nichols, *Trans. ASME*, 64, 759–768 (1942).

OTHER RESOURCES

For a more detailed analysis of the root locus method, see the reference below, which gives design rules and applications.

Douglas, J., *Process Dynamics and Control, Vols. I and II*, Prentice-Hall, Englewood Cliffs, NJ, 1972.

The next two references give further details on frequency response. The first is introductory, and the second uses more challenging mathematical methods.

Caldwell, W., G. Coon, and L. Zoss, *Frequency Response for Process Control*, McGraw-Hill, New York, 1959.

MacFarlane, A. (ed.), *Frequency-Response Methods in Control Systems*, IEEE Press, New York, 1979.

The following references present some historical background and some of the key milestones in control systems engineering.

MacFarlane, A., "The Development of Frequency Response Techniques in Automatic Control," *IEEE Trans. Auto Contr.*, AC-24, 250 (1979).

Oldenburger, R. (ed.), *Frequency Response*, Macmillan, New York, 1956.

The stability of a nonlinear system in a defined region can be determined for some systems and regions using the (second) method of Liapunov, which is presented in Perlmutter (1972) and

LaSalle, J., and S. Lefschetz, *Stability of Liapunov's Direct Method with Applications*, Academic Press, New York, 1961.

The methods introduced in this chapter provide a theoretical basis for determining the effects of all elements in the feedback loop, process, instrumentation, and control algorithm on stability and tuning. These questions ask you to apply these methods.

QUESTIONS

- 10.1.** Consider the three-tank mixing process with a proportional-only controller in Example 10.5. Recalculate the root locus for the case with the three tank volumes reduced from 35 to 17.5 m³. Determine the controller gain for a proportional-only algorithm at which the system is at the stability limit. Compare your result with Example 10.5 and discuss.
- 10.2.** Example 10.4 established the stability of a system when operated at a temperature $T = 320$ K. Given the expression for the reaction rate constant of $k = 6.63 \times 10^8 e^{-6500/T} \text{ min}^{-1}$, determine if the system is stable at 300 K and 340 K. Explain the trend in your results and determine which of the three cases is the worst case from a stability point of view.
- 10.3.** Answer the following questions, which revisit the interpretations (I–VI) in Section 10.8.
 - (a) (I) For the process in Example 5.2, determine the PI controller tuning constants using the Ziegler-Nichols closed-loop method. The manipulated variable is the inlet feed concentration, and the controlled variable is (i) Y_1 , (ii) Y_2 , (iii) Y_3 , and (iv) Y_4 . Answer for both cases 1 and 2 in Example 5.2.
 - (b) (II) Discuss the effect of the derivative mode on the stability of a closed-loop control system. Explain the results with respect to a Bode stability analysis.
 - (c) (III) A linearized model is derived for the process in Figure 9.1. The model is to be used for controller tuning. Model errors are estimated to be 30 percent in L , V , and F_B , and they can vary independently. Estimate the worst-case dynamic model that is possible within the estimated errors.
 - (d) (IV) Assume that experimental data indicates that a closed-loop PI system experienced sustained oscillations with constant amplitude at specified values of their tuning constants K'_c and T'_I . Estimate proper, new values for the tuning constants.
 - (e) (V) Determine the range of tuning constant values that result in stability for the following systems and plot the region with K_c and T_I as axes. Locate good tuning constant values within this region: (1) the level system in Example 10.1 for P-only and PI controllers; (2) the three-

tank mixing system with a PI controller; (3) Figure 9.1 with $\theta = 5$ and $\tau = 5$.

- (f) (VI) Using arguments relating to stability and Bode plots, determine model simplifications in the system in Figure 7.1 and Table 7.2, to give the lowest-order system needed to analyze stability and tuning with acceptable accuracy.

- 10.4.** Given the process reaction curve in Figure Q10.4, calculate initial PID controller tuning constants using the Ziegler-Nichols tuning rules. Compare the results to values from the Ciancone correlations and predict which set of values would provide more aggressive control.

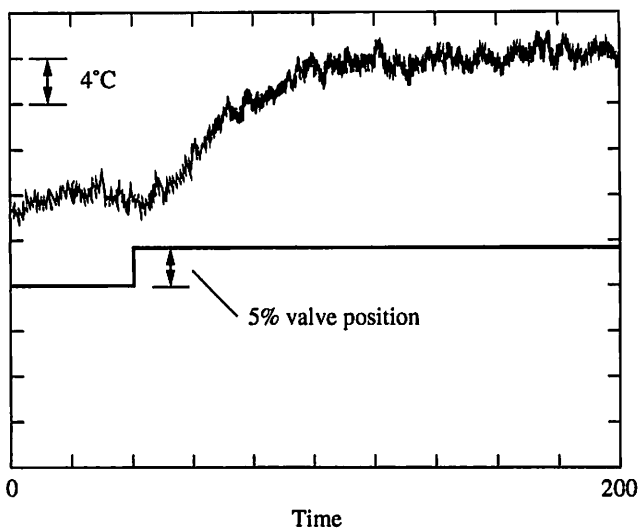


FIGURE Q10.4

- 10.5.** Given a feedback control system such as the three-tank mixing process, determine the effect of the following equipment changes on the tuning constants.

- (a) Installing a faster-responding control valve.
- (b) Installing a control valve with a larger maximum flow.
- (c) Installing a faster-responding sensor.

- 10.6.** Without calculating the exact values, sketch the Bode plots for the following transfer functions using approximations:

$$(a) G_{OL}(s) = \frac{5.3}{4.5s + 1} \quad (b) G_{OL}(s) = \frac{1}{5s} \quad (c) G_{OL}(s) = \frac{2.0e^{-2s}}{(3s + 1)^2}$$

- 10.7.** Determine the root locus plot in the complex plane for controller gain of zero to instability for the following processes: (a) example heater in Section 8.7; (b) Example 10.1; (c) Example 10.8. For the systems with PI controllers, assume that the integral time is fixed at the value in the original solution.

- 10.8.** (a) Is the Bode stability criterion necessary, sufficient, or necessary and sufficient?

- (b) Is it possible to determine the stability of a feedback control system with non-self-regulating process using the Bode stability criterion?
- (c) Explain the limitations on the process transfer function imposed for the use of the Bode method.
- (d) Determine the stability of the system in Example 10.4 using the Bode method.

10.9. Confirm the expressions for the amplitude ratios and phase angles given in Table 10.2.

10.10. Prove the following statements and give an explanation for each in your own words by referring to a sample physical system.

- (a) The phase lag for a gain is zero.
- (b) The amplitude ratio for a first-order system goes to zero as the frequency goes to infinity.
- (c) The amplitude ratio for a second-order system with a damping coefficient of 0.50 is not monotonic with frequency.
- (d) The phase angle decreases without limit as the frequency increases for a dead time.
- (e) For an integrator, the amplitude ratio becomes very large for low frequencies and becomes very small for large frequencies.
- (f) The amplitude ratio for a PI controller becomes very large at low frequencies.

10.11. For each of the physical systems in Table Q10.11, explain whether it can experience the dynamic responses shown in Figure Q10.11 for a step input (not necessarily at $t = 0$). The systems are to be considered idealized;

TABLE Q10.11

System	Input variable (separate answer for each)	Output variable (separate answer for each)	Control (separate answer for each)
Figure 7.1 and Example 7.1	Signal to value	Measured temperature	None
Example 8.5	Set point	Tank temperature	(i) P-only (ii) PI
Reactor in Section C.2	F_c	Reactor temperature	None
Example I.2	(i) F_s (ii) F_A	(i) C_{A1} , (ii) C_{A2}	None
Example 3.3	(i) C_{A0} (ii) F	(i) C_{A1} , (ii) C_{A2}	None
Example 9.1	Set point	C_A	PID
Example 7.2	(i) Signal to valve (ii) Set point of controller in Example 9.2	(i) C_{A1} , (ii) C_{A2} , and (iii) C_{A3}	(i) None (ii) P-only (iii) PI

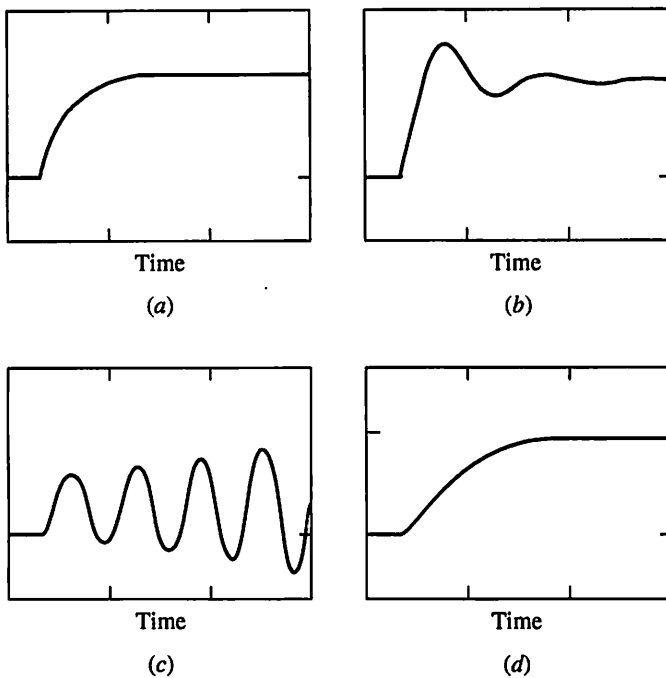
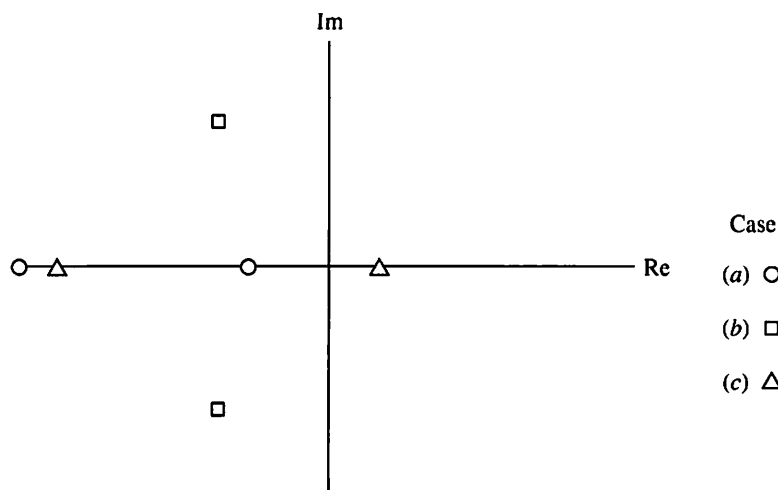


FIGURE Q10.11

in other words, the mixing is perfect, final element and sensor dynamics are negligible unless otherwise stated, and so forth. Provide quantitative support for each answer based on the model structure of the system.

- 10.12.** The Bode stability technique is applied in this chapter to develop the Ziegler-Nichols closed-loop tuning method. For each of the following changes describe an appropriate modification to the closed-loop Ziegler-Nichols tuning method. Answer each part of this question separately.
- The controller used in the plant calculates the error with the sign inverted; $E = CV - SP$.
 - The linear plant model identified using a process reaction curve also has an estimate of the uncertainty in its feedback model parameters, K_p , θ , and τ .
 - The process model, in addition to parameters for the feedback process, has estimates of the disturbance dead time and time constant.
- 10.13.** The stability analysis methods introduced in this chapter are for linear systems, which give local results for nonlinear systems. What conclusions can be drawn from the linear analysis at the extremes of the ranges given about the stability of the following systems? (a) Example 9.4 with F_B varying from 6.9 to 5.2 m^3/min and (b) Example 9.1 with the volume of the tank and pipe varying by $\pm 30\%$.
- 10.14.** Given the systems with roots of the characteristic equation shown in Figure Q10.14, sketch the transient responses to a step input for each, assuming the numerator of the transfer function is 1.0.
- 10.15.** Prove all of the statements in Table 10.3.

**FIGURE Q10.14**

10.16. Answer the following questions regarding the derivative mode.

- (a) Based on the Bode plot of a PID controller, what is the effect of high-frequency measurement noise on the manipulated variable?
- (b) Redraw Figure 10.13h for $T_d = T_I/4$.
- (c) We have considered a PID controller that uses error in the derivative for the stability analysis. However, the controller algorithm used commonly in practice uses the controlled variable in the derivative mode. How should the stability analysis be altered to account for the use of the controlled variable in the derivative?

10.17. Consider the three-tank mixing process in Example 7.2 with the same three 5-minute time constants and with a transportation delay of 4.3 min between the mixing point and the entrance to the first tank.

- (a) Calculate initial tuning parameters using the Bode stability method and the Ziegler-Nichols correlations.
- (b) Explain the changes in the tuning constant values from those in Example 10.10.
- (c) Would you expect the control performance for the system with transportation delay to be better or worse than the system without transportation delay?

10.18. (a) The dynamic performance of the system in Example 10.10 was deemed too oscillatory with the initial tuning calculated via Ziegler-Nichols correlations. How would you change the tuning constants, which constants, and by how much to achieve reasonably good performance with little oscillation?

(b) Given the results in Example 10.13 which showed that the Ziegler-Nichols tuning correlations do not seem to yield robust control performance for low fraction dead time, how would you modify the Ziegler-Nichols correlations for $\theta/(\theta + \tau) < 0.2$?